Fakultät für Medizin

Defective Skeletal Myogenesis after Genomic Aldehyde Dehydrogenase 1 Knockout:

Isoform ALDH1A1 and ALDH1A3 Proteins are Essential for Myotube Formation

Laura Sophie Rihani

Vollständiger Abdruck der von der promotionsführenden Einrichtung
Medical Graduate Center, Fakultät für Medizin der Technischen Universität München
zur Erlangung des akademischen Grades eines Doktors der Naturwissenschaften
genehmigten Dissertation.

Vorsitzender: Prof. Dr. Simon N. Jacob

Prüfende der Dissertation:

1. Prof. Dr. Jürgen Schlegel
2. Prof. Dr. Gabriele Multhoff

Die Dissertation wurde am 09.07.2020 bei der Technischen Universität München eingereicht und durch die Fakultät für Medizin am 06.10. 2020 angenommen.

Table of contents

Abbreviations

1a1 V	Recombinant ALDH1a1 overexpression vector
1a3 V	Recombinant ALDH1a3 overexpression vector
ALDH	Aldehyde Dehydrogenase
ALDH1A1	Human Aldehyde Dehydrogenase 1A1
ALDH1A3	Human Aldehyde Dehydrogenase 1A3
ALDH1a1	Non-human Aldehyde Dehydrogenase 1a1
ALDH1a3	Non-human Aldehyde Dehydrogenase 1a3
AMP	Ampicillin
APS	Ammonium Peroxodisulfate
ATCC	American Type Culture Collection
BAAA	BODIPY-aminoacetaldehyde
BAA	BODIPY-aminoacetate
BB	Back Bone
BLAST	Basic Local Alignment Search Tool
BSA	Bovine Serum Albumin
C.P.	Cancelled Production
CDK	Cyclin-dependent kinase
Ctrl	Control
D	Days
DAB	Diaminobenzidine
DAPI	4′ ,6-Diamidin-2-phenylindol
DEAB	4-Diethylaminobenzaldehyde
Diff	Differentiation

DM	Differentiation Medium
DMEM	Dulbecco's Modified Eagle's Medium
DMSO	Dimethyl Sulfoxide
DNA	Deoxyribonucleic acid
DSF	Disulfiram
DMD	Duchenne's Muscle Dystrophy
DTT	Dithiothreitol
E. coli	Escherichia Coli
FACS	Fluorescence Activated Cell Sorter
FBS	Fetal Bovine Serum
FCS	Fetal Calf Serum
FITC	Fluorescein Isothiocyanate
FSC	Forward Scatter
GFP	Green Fluorescent Protein
HRP	Horseradish Peroxidase
HS	Horse serum
IF	Immunofluorescence
KO	Knockout
NEB	New England Biolabs
G418	Neomycin
ORF	Open Reading Frame
PAX	Paired-box Protein
PBS	Phosphate Buffered Saline
PM	Proliferationmedium
RA	Retinoic Acid

ROS	Reactive Oxygen Species
RMS	Rhabdomyosarcoma
RT	Reverse transcription-polymerase chain reaction
SC	Satellite cell
SDS-PAGE	Sodium Dodecyl Sulfatepolyacrylamidgel Electrophoresis
sgRNA	Single-guide Ribonucleic Acid
SSC	Sideward Scatter
KO	Knockout
OEV	Overexpression
OS	Oxidative stress
Q2	Quarter 2
WB	Western Blot
W/O	Without
WT	Wildtype

A. Summary

INTRODUCTION Satellite cells (SC) are the stem cell population of skeletal muscle and constitute the resource for muscle growth. SC action relies on environmental stimuli, such as physical activity, insult or oxidative stress. Interestingly, the enzyme Aldehyde Dehydrogenase 1 (ALDH1) is not only a functional determinant in retinoic acid (RA) signaling and subsequent differentiation, but also in the process of antioxidative reaction. It could be recently demonstrated that isoforms ALDH1A1 and ALDH1A3 are co-localized in SCs of human skeletal muscle tissue. ALDH1 is an important factor for cell growth, regenerative action and cell maintenance. Moreover, ALDH1 was previously identified as hallmark for subpopulations of muscle progenitor cells with high myogenic capacity and better resistance to oxidative stress. Although, ALDH1 activity has been addressed in several experimental studies, the functional role of ALDH1A1 and ALDH1A3 in myogenesis remains indistinct. **METHODS** Using human RH30 and murine C2C12 myoblast cells myogenic development was analyzed in regard of enzyme ALDH1 isoforms ALDH1A1 and ALDH1A3 functions. Wildtype cells were compared with genomic ALDH1A1 and ALDH1A3, respectively, knockout C2C12 and RH30 cells. Moreover, chemical ALDH inhibition as well as opposed condition of recombinant ALDH1A1 and ALDH1A3 overexpression was included. **RESULTS** Here, I could demonstrate the functional mechanism of isoforms ALDH1A1 and ALDH1A3 in myogenic myotube formation. Increased ALDH1 activity and ALDH1A1 and ALDH1A3 isoform protein levels were predominant in differentiation. Interestingly, enzymatic ALDH inhibition caused accumulated protein levels of ALDH1A1 and ALDH1A3 and induced differentiation. Recombinant overexpression of isoforms ALDH1A1 and ALDH1A3, respectively, accelerated protein levels of ALDH1A1 and ALDH1A3 as well and lead to subsequent differentiation. Protein accumulation of ALDH1A1 and ALDH1A3 seemed to be important for differentiation, therefore genomic knockout of ALDH1A1 and ALDH1A3, respectively, was performed and demonstrated a deficient differentiation phenotype despite the presence of serum-

withdrawal. Recovery of differentiation process in knockout cells could be shown by re-transfection of recombinant ALDH1A1 and ALDH1A3, respectively. **CONCLUSION** Findings show, that isoform ALDH1A1 and ALDH1A3 proteins are essential in the process of myogenic differentiation, since ALDH1A1 knockout and ALDH1A3 knockout, respectively, lost their potential to differentiate. Recombinant re-expression of ALDH1A1 and ALDH1A3, respectively, in ALDH1 isoform knockout cells recovered myogenic differentiation. Most interestingly, chemical inhibition of enzymatic activity leads to protein upregulation of ALDH1A1 and ALDH1A3 and consequent myogenic differentiation. Results demonstrate the importance of ALDH1A1 and ALDH1A3 in myogenic differentiation and may constitute a favorable activator of SCs.

B. Introduction

Satellite cells (SC) constitute the stem cell population of skeletal muscle and the resource of myogenic growth. Regulatory stimuli, such as physical activity or insult, inflammation and oxidative stress induce SC activation for adaptive growth and regeneration (Forcina et al., 2019). Therefore, SC action aims for both muscle growth and cellular maintenance.

SC behavior and the process of myogenesis have been addressed in several experimental studies (Cobb, 2013; Shen et al., 2003), that identified characteristic markers of quiescent or activated SCs and established markers for myogenic proliferation and differentiation. Although the influence of stimuli on SC activation and myogenic growth are part of several experimental investigations (Mukund & Subramaniam, 2020; Pownall et al., 2002), potential SC activators and their functional role in differentiation are not yet characterized.

Interestingly, enzyme aldehyde dehydrogenase 1 (ALDH1), in particular its isoforms ALDH1A1 and ALDH1A3, oxidize in the vitamin A signaling pathway retinaldehyde into the metabolite retinoic acid, which then regulates differentiation (Gudas, 2012). Moreover, ALDH1 is known for its antioxidative function in the protection against oxidative stress products (Jean et al., 2011). Most recently, I was able to demonstrate the co-localization of isoforms ALDH1A1 and ALDH1A3 in SCs of human skeletal muscle tissue (Rihani et al., submitted data). Several studies also emphasized ALDH1 as hallmark of a myoblast subpopulation with high myogenic capacity and better resistance to oxidative stress (Vauchez et al., 2009; Vella et al., 2011). In addition, ALDH1 avoids DNA damage, mitochondric dysfunction and apoptosis (Schieber & Chandel, 2014; Singh et al., 2013). Conclusively, the ALDH1 seems to play an important role in SC maintenance and myogenesis. Therefore, the implementation of a detailed analysis of ALDH1 function in SCs and myogenesis is of high interest.

In the following chapters basic traits about human skeletal muscle biology, the process of myogenesis and satellite cell action are introduced. In addition, enzyme ALDH is described in the context of RA signaling and oxidative stress scavenging.

1. Biology of Skeletal Muscle

40% of human body weight can be accounted to striated skeletal muscle tissue. Skeletal musculature consists of various compartments (Figure 1), such as single fibers, which can be divided into fibrils and subsequently in filaments. Each fiber is covered with sacroplasmatic reticulum and every muscular compartment has capillaries of blood vessels and nerve fibers, extending along the tissue to provide energy and oxygen intake as well as nerval innervation.

Regenerative processes are conducted by muscle stem cells, known as satellite cells (SC). The term “satellite cell” is owed to its anatomical localization between the sarcolemma and basal lamina of its resident myofiber.

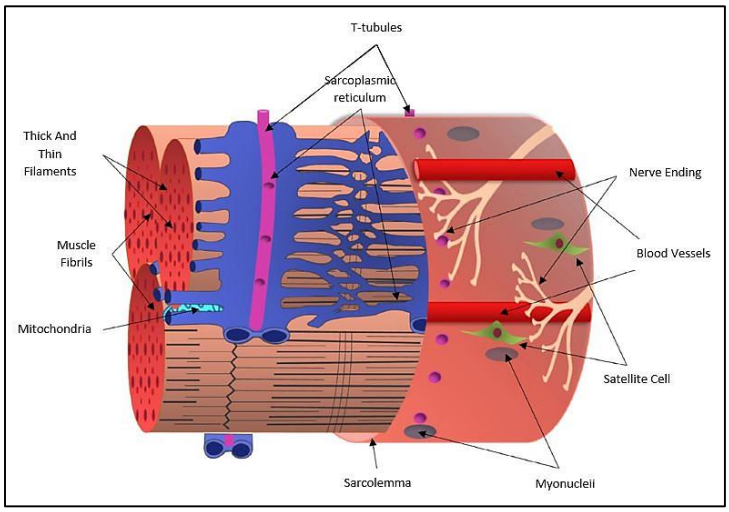

Figure 1: Skeletal muscle fiber compartments (modified version from Mukund & Subramaniam, 2020)

1.1. Satellite Cells

SCs are considered as the important factor for cell maintenance, repair and growth of skeletal muscle tissue. A unique characteristic of stem cells is the ability to return to quiescent status after being active and performing cell division (Yablonka-Reuveni, 2011). In regard of skeletal muscle tissue being a terminally differentiated organ, SCs are the important factor for muscle growth and regeneration. The process of muscle formation is described as process of myogenesis.

Typically, SCs are in a quiescent state, but can be activated by environmental stimuli for proliferation and differentiation behavior (Mukund & Subramaniam, 2020). SC function can be divided into symmetric division for self-renewal and consecutive restock of the SC pool or further proliferation for muscle tissue growth and asymmetric division of SCs aims for myotube formation described as differentiation process (Forcina et al., 2019).

SC function is regulated by environmental stimuli (Figure 2). For instance, injury, inflammation and oxidative stress impair muscular structures and cause SC activation for regeneration (Mukund & Subramaniam, 2020). If the process of protein degradation is higher than protein synthesis muscle structures become atrophic (Schiaffino et al., 2013), but it was shown that anti-inflammatory treatment positively influences the effectiveness of regenerative activity (Mackey et al., 2016). Moreover, physical activity and repetitive movements regulate SC activation for growth (Zuo & Pannell, 2015) and the expansion of the SC pool (Shefer et al., 2013). In human skeletal muscle the adaptive response of SCs to exercise is a frequently used model for investigation of SC action and physiological regulation (Snijders et al., 2015). Nonetheless, it is controversially discussed if mechanical and inflammatory signals independently drive SC-induced hypertrophic growth (Bert Blaauw & Carlo Reggiani, 2014).

In general, SC function describes the process of regenerative and adaptive growth and is dependent on environmental stimuli change (Tierney & Sacco, 2016).

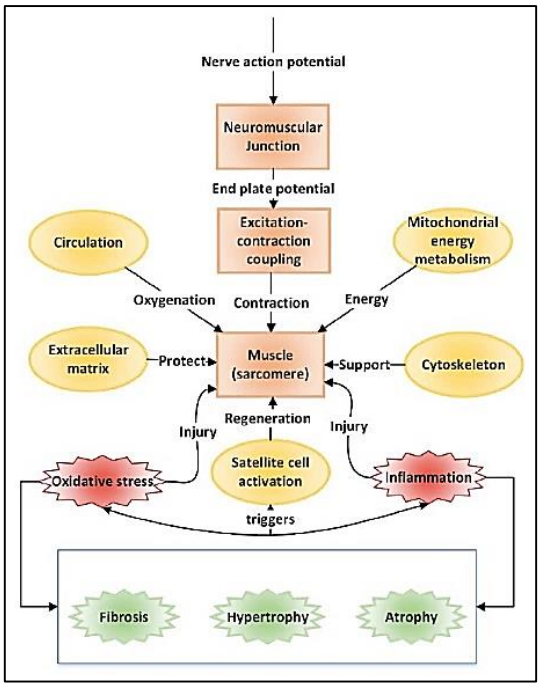

Figure 2: Functional network of skeletal muscle biology (modified version from Mukund & Subramaniam, 2020)

1.2. Myogenesis

Paired-box protein Pax3- and Pax7-positive precursor cells develop among others into myogenic SCs with particular Pax7 expression (Feng et al., 2018; Y. X. Wang & Rudnicki, 2011).

Moreover, SCs can be identified by both myogenic transcription factors and cell cycle stage-dependent gene expression markers (Figure 3). Activated SCs enter the process of myogenic development, which is modulated by the expression of myogenic regulatory factors (MRFs), MyoG1, MyoD, MRF4 and MYF5 (Pownall et al., 2002). Therefore, proliferating myoblasts express MYF5 and MyoD, whereas MyoG- and MEF2-upregulation induces differentiation and transforms myoblasts into myocytes (Figure 3) (Moran et al., 2002). Consecutive MRF4 expression modulates myotube formation with decreasing levels of MyoG (Mukund & Subramaniam, 2020).

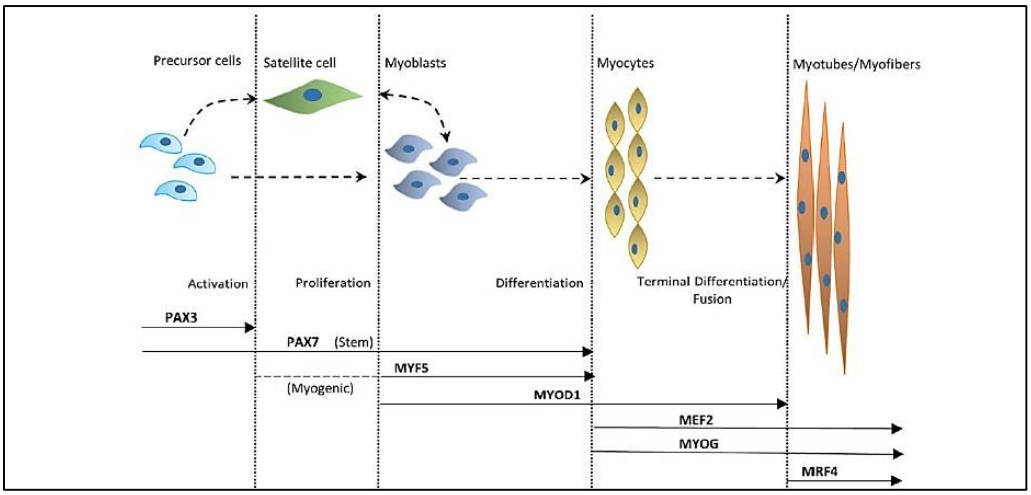

Figure 3: Myogenic transcription factors in skeletal muscle development (modified version from Mukund & Subramaniam, 2020)

Myogenic development can be traced by the analysis of cell cycle status related gene expression patterns (Cobb, 2013, Figure 4). For instance, p21WAF/ Cip1 inhibits G1 CDK complexes (cyclin-dependent kinase) and induces subsequent cell cycle phase. Subsequently, cells can either enter G1 for proliferation as myoblasts, switch post G2 and M-phase back to quiescent G0 status or continue developmental process to terminally differentiate into myotubes.

The combination of myogenic transcription factors and cell cyle-dependent markers enables a comprehensive analysis of myogenic development. For instance, MyoD expression modulates p21, which inhibits CDK activity upon myotube formation and is therefore, describing proliferation arrest (Guo K. et al., 1995).

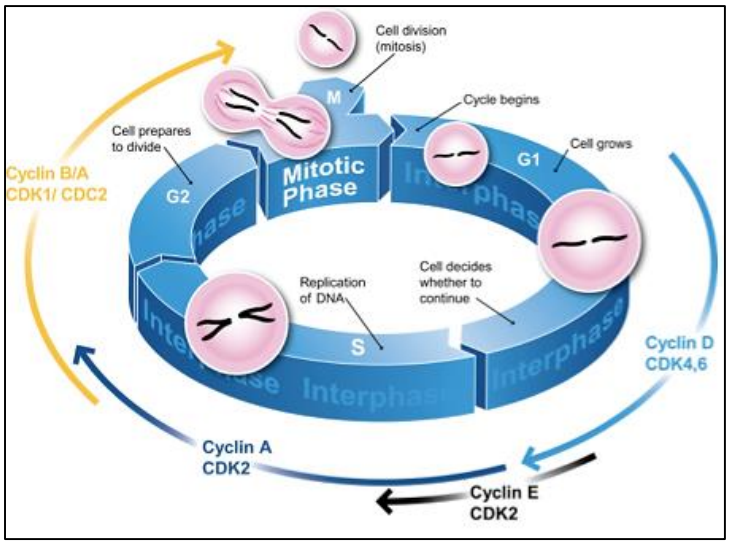

Figure 4: Myogenic gene expression in cell cycle stages, from Cobb, 2013

In addition to myogenic transcription factors and cell cycle-dependent markers, specific membrane proteins can be used for SC labeling (Figure 5). Recently, Etienne et al., 2020, identified in human SCs a subpopulation of CD56/Ncam1 positivity and CD34 negativity with high myogenic capacity and increased resistance to oxidative stress. Application of all types of labels contributes to a more specific characterization of SCs by expression pattern analysis and is also demonstrated in Montarras et al., 2013 and Y. X. Wang et al., 2014.

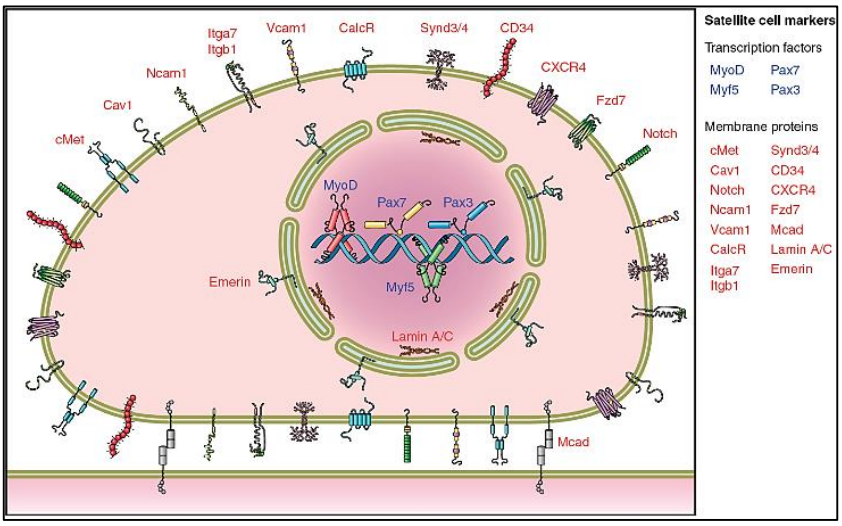

Figure 5: Schematic satellite cell expression profile, from Hang Yin et al., 2013

1.3. Senescence

Findings show a reduced growth factor concentration over the lifespan with an increased katabolic process in skeletal muscle tissue (Larsson et al., 2018). Resulting sarcopenia can be described as progressive skeletal muscle mass and strength loss (Emanuele Marzetti et al., 2017). Studies demonstrated that resistance training is a useful antagonist for muscle tissue degradation and prolongs muscle repair processes (Wackerhage, 2017). Nevertheless, progressive sarcopenia impairs anti-inflammatory reaction and promotes cellular senescence (Nelke et al., 2019).

Senescent cells depict a permanent state of cell cycle arrest and loss of apoptosis (Hernandez-Segura et al., 2018). Further, senescent cells are contributors of decreased regenerative capacity and increased inflammation (Kirkland & Tchkonia, 2017), which again promotes sarcopenia. Senescent behavior in SCs can be observed by increased dysfunction in regenerative action (García-Prat et al., 2013; Thornell, 2011) and tend to switch into senescent status instead of quiescence (Sousa-Victor et al., 2014). Environmental stressors like high levels of oxidative stress enhance the cellular process of aging and induce senescent cell behavior (van Deursen, 2014). It was shown that artificially reduced p38α MAPK stress response signaling demonstrated a higher longevity of myogenic progenitor cells (Papaconstantinou et al., 2015). Senescence can be delayed in muscle cells by effective scavenging of high intracellular stress levels over life time (Benjamin D Cosgrove et al., 2014).

The mechanism of autophagy was identified as a determining factor in muscle cells for senescence prevention (Wen & Klionsky, 2016) and is also currently discussed as activating trigger of quiescent cells (Rajendran et al., 2019). Moreover, it was shown that physical activity modulates autophagy and enhances cellular homeostasis in skeletal muscle (Vainshtein & Hood, 2016). The function of autophagy in SCs has been described as promoting factor for longevity, including delayed senescent behavior (Fiacco et al., 2016; García-Prat et al., 2016).

1.4. Experimental Skeletal Muscle Cells

In vitro analysis of SC-like muscle cells allows an investigation of treatment-dependent myogenic behavior within a controllable working system. Gathered findings improve the identification of novel approaches in skeletal muscle therapy and the examination of skeletal muscle biology in general.

The isolation of muscle cells from skeletal muscle tissue and SC-marker specific cell sorting enables the establishment of a purified subpopulation with confined expression patterns (Ding et al., 2017; Etienne et al., 2020; Motohashi et al., 2014). Unfortunately, primary cell culture only achieves a maximum of 20 passages within active proliferation and then switches to senescent behavior (Wei et al., 2011). Repeated experiments in the same primary culture is therefore aggravated.

In contrast, immortalized myoblast cell lines enable a time-independent examination of myogenesis and are widely accepted as SC-like models. For instance, murine C2C12 myoblasts were investigated in regard of myotube formation (Portiér et al., 1999) and for approval of pre-established markers of transcription factors, cell cycle–dependent genes as well as membrane markers (Shen et al., 2003), where proliferation (Myf5) and differentiation (Myogenin, α-Aktin) could be successfully demonstrated (Figure 6). Moreover, a conclusive insight in the process of hypertrophy in C2C12 myoblasts was demonstrated and the analysis revealed an increased activation of cell cycle G1-phase (Hlaing et al., 2002).

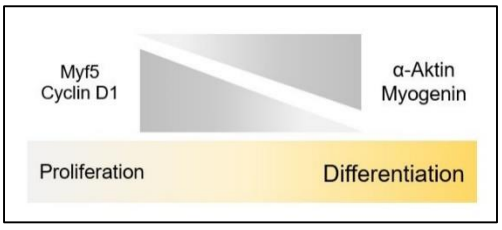

Figure 6: Expression profile of C2C12 in the process of differentiation

As part of my Master's thesis, C2C12 differentiation was examined using priory mentioned markers of myogenic transcription factors and cell cycle stages in Western Analysis and depicted a reliable differentiation model. Furthermore, the protein level of Aldehyde Dehydrogenase 1, which will be discussed in chapter 2, was initially analyzed in C2C12.

2. Aldehyde Dehydrogenase

Aldehyde Dehydrogenase (ALDH) constitutes an enzyme superfamily with recently 19 identified genes complying various functions (Black et al., 2009). Since ALDH superfamily demonstrates a variety of functions a brief overview of the most interesting families is given (Figure 7).

ALDH2 family is known as detoxifying agent in alcohol metabolism of the liver and was recently discussed as promising target for alcoholic liver disease therapy (W. Wang et al., 2020). Furthermore, studies suggested differences in the prevalence of ALDH2 isoforms among human ethnic groups like Asian, Caucasian and African with subsequent variances in alcohol permissiveness and dependence (Wall et al., 2016).

In the 1950s ALDH inhibitor Antabuse (Disulfiram) was applied in alcohol-dependent patients for alcohol withdrawal (Moriarty, 1950). Maintained ALDH dysfunction through drug treatment increased the sensitivity to alcohol consumption and should facilitate deprivation. Though, Antabuse has been contra indicative in patients with psychosis, diabetes mellitus, epilepsy, cardiovascular diseases and brought up side effects as confusion and hyptension (Amuchastegui et al., 2014).

In contrast, Disulfiram treatment is of high interest for cancerous growth inhibition by ALDH positive cancer cell targeting (Jin et al., 2018; Lin & Lin, 2011). Furthermore, Antabuse is applied in clinical cancer therapy, since ALDH1 isoform ALDH1A3 was found to be highly

expressed in recurrent glioblastoma brain tumors and being responsible for the resistance to chemotherapeutic drug Temozolomide (Jiayi Huang et al., 2019).

The active role of ALDH1 isoform was examined as cancer cell-protective agent in oxidative stress situations and as averting factor of cell death in recent studies, like in rhabdomyosarcoma (Monti & Fanzani, 2016), isoform ALDH1A2 in pathogenesis of T-cell acute lymphoblastic leukemia (T-ALL) (Zhang et al., 2020) and isoform ALDH1A1 in lung adenocarcinomas (Lei et al., 2019).

A partial overview of ALDH isoform functions is depicted in Figure 7.

Human *ALDH* genes and gene products

Gene	Protein Description
ALDH1A1	ALDH1A1 is a cytosolic enzyme that oxidizes retinal, acetaldehydes and 3-deoxyglucosone (a product of protein deglycation and a potent glycating agent).
ALDH1A2	ALDH1A2 is a cytosolic enzyme that is integrally involved in the oxidation of retinal to retinoic acid during embryonic development. *Aldh1a2(-/-)* mice are embryolethal.
ALDH1A3	ALDH1A3 is a cytosolic retinaldehyde-metabolizing enzyme.
ALDH1B1	ALDH1B1 is a mitochondrial enzyme that metabolizes acetaldehyde.
ALDH1L1	ALDH1L1 is a fusion protein comprising three domains: a formyl transferase domain at the amino terminal, a centrally-located formyltransferase carboxyl terminal domain and an aldehyde dehydrogenase domain at its carboxyl terminal (Figure 2).
ALDH1L2	ALDH1L2 shares ≈73% identity with ALDH1L1; no functional data have been reported for this protein.
ALDH2	ALDH2 is a mitochondrial enzyme involved in the oxidation of acetaldehyde and the metabolites of dopamine and norepinephrine,

Figure 7: Human ALDH genes and function, modified version from Black et al., 2009,

In this study most emphasis will be placed on ALDH1 family, since it regulates retinoic acid (RA) metabolism and consecutive differentiation (Vassalli, 2019) and moreover, a protective scavenger of free aldehydes (Singh et al., 2013). ALDH1 is beneficial for tumorous and non-tumorous cell maintenance (Tomita et al., 2016) and is thus, an active part in processes of growth and cellular protection. In the following paragraphs ALDH1 activity will be discussed in regard of RA signaling pathway and oxidative stress reaction.

Of note, human isoforms of ALDH families are entitled with capital A, i.e. ALDH1 A1, A3, whereas non-human isoforms are written with a small letter a, i.e. ALDH1 a1, a3. In this work both spellings are regarded as equal, since a comprehensive view on enzyme ALDH regardless the species is collected and to simplify the description and discussion of gathered results.

2.1. Retinoic Acid Metabolism

The role of ALDH1 in RA signaling is the conversion step of retinaldehyde in RA. In 2012 Gudas, entitled the isoforms ALDH1A1, -1A2 and -1A3, respectively, as key players in this step (Figure 8). Activation of transcriptional factors of primary target genes for differentiation is dependent on the degree of RA concentration and therefore, subordinated to ALDH activity.

In detail, the metabolism of vitamin A describes the conversion of retinol to retinaldehyde with consecutive metabolite generation of retinoic acid (RA) (Figure 8) (D'Ambrosio et al., 2011). RA is known to be stored in many cell types and plays an important role in the induction of differentiative cell behavior (Gudas, 2012). Through stimuli-dependent differentiation is regulated by RA entering the nucleus and binding to retinoic acid receptors (RAR). Growth behavior is triggered by downstream target genes including Akt through binding to RXR inside the nucleus, and RARα outside the nucleus (Alric et al., 1998). Differentiation is induced through triggering downstream target genes by RARβ. (Figure 9) For instance, in experimental C2C12 muscle cells it could be shown that, RA signaling is promoting differentiation after serum-withdrawal (Albagli-Curiel et al., 1993).

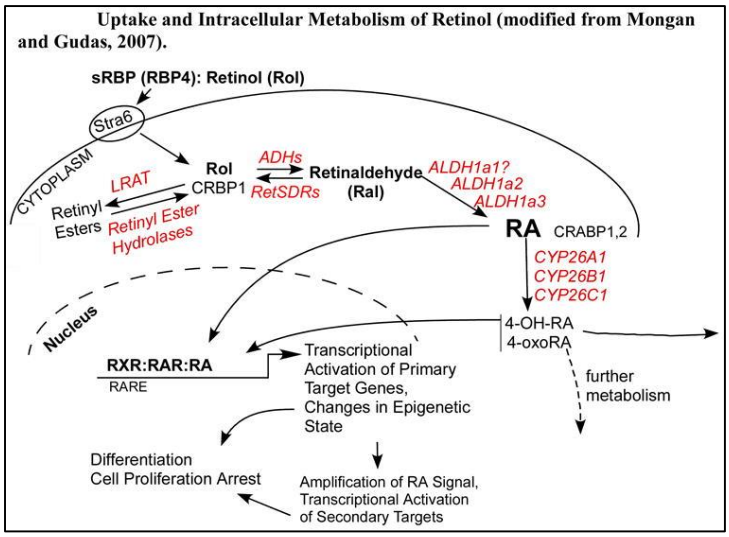

Figure 8: Retinoic Acid Pathway, from Gudas, 2012

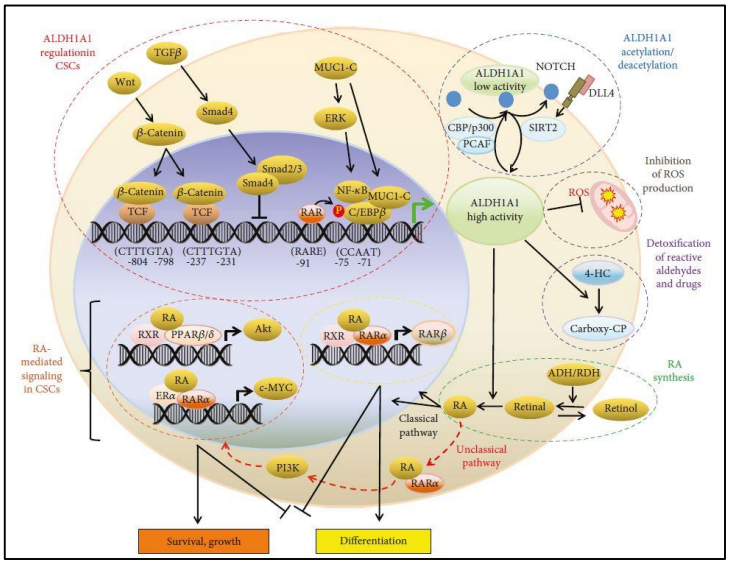

Figure 9: ALDH: regulation and functional effects, from Vassalli, 2019

Since cancers are mostly considered as ALDH positive and resistant to oxidative stress, the mechanism of RA induced differentiation was investigated for cancer therapy (Barlow et al., 2006; Crouch & Helman, 1991; Soprano et al., 2007). For instance, Liu et al., 2016 demonstrated a loss of proliferation potential by enzymatic ALDH1A1 inhibition in non-small cell lung cancer (NSCLC) stem cells.

Conclusively, ALDH1 isoforms regulate differentiation by RA metabolism and harbor the to modulate on of the basic traits in muscle cell development.

2.2. Oxidative Stress

Oxidative stress (OS) describes an accumulation of pro-oxidants, known as reactive oxygen species (ROS) and was mentioned before in chapter 1.3. in the context of cellular aging (van Deursen, 2014).

OS causes inflammatory immune reactions, cellular membrane and DNA damage, dysfunctional mitochondria and apoptotic cell behavior (Figure 10). Identified inducers of OS (Figure 10) are injury and hypoxic conditions such as smoking, radiation or heat shock (Kozakowska et al., 2015; Sin et al., 2013). High levels of OS negatively affect muscle tissue homeostasis and promote the process of aging, whereas low levels of OS positively influence muscle cell growth as mentioned before in chapter 1.1. in the context of physical activity (Musarò et al., 2010; Nelke et al., 2019).

The process of OS describes the intracellular accumulation of ROS, which activates lipid peroxidation (LP). The LP mechanism reduces ROS levels and is measurable through MDA (malondialdehyde) generation, a known product of LP. MDA measurement enables alternative oxidative stress estimation and is depicting a useful marker of disease risk, since ROS levels are rather low and short-living (Ito et al., 2019). MDA refers to the group of free aldehydes generating non-enzymatic free radicals and often target lipids and lipoproteins of membranes (Figure 10, Figure 1Figure 11, Fritz & Petersen, 2013). Therefore, DNA and mitochondria are commonly damaged.

OS reaction is also discussed as a response to cancerous diseases (Takaki et al., 2019) and facilitates mutations and pathological cell behavior.

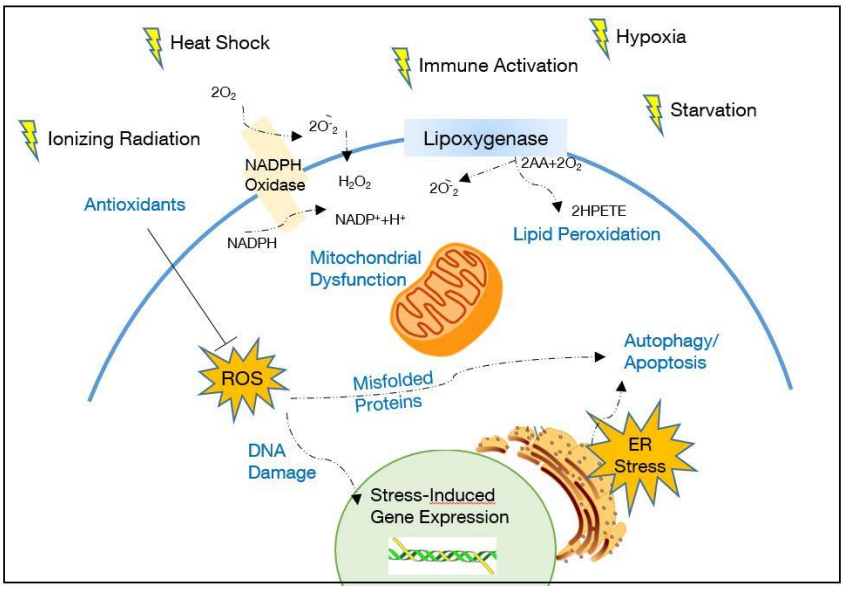

Figure 10: Oxidative stress reaction (modified version from online information, https://www.enzolifesciences.com/platforms/cellular-analysis/oxidative-stress, 1st 07 2020)

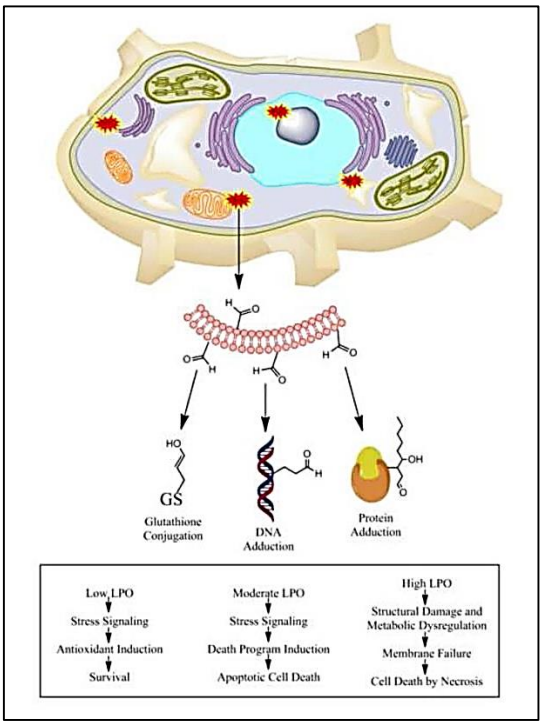

Figure 11: Cellular effects of oxidative stress and lipid peroxidation, from Fritz & Petersen, 2013

Among antioxidants enzyme ALDH is an antioxidative agent in oxidative stress detoxification (Singh et al., 2013) and is therefore, functionally active for cellular maintenance. Consecutive stimuli-driven regenerative processes are induced and SCs accomplish skeletal muscle cell repair. The activation of SCs through environmental stimuli is implied but the detailed functional mechanism of ALDH in SC activation remains mostly unclear.

C. Objective

The process of myogenic growth and differentiation is reliant on the action of satellite cells (SCs), which constitute the stem cell population in skeletal muscle. SCs activation is dependent on physiological regulation and the demand of regenerative activity (Vella et al., 2011).

The enzyme Aldehyde Dehydrogenase 1 (ALDH1), in particular its isoforms ALDH1A1 and ALDH1A3, respectively, are not only regulating retinoic acid (RA) metabolism and differentiation, but also detoxify oxidative stress products and protects cells from damage. The central position of ALDH1 activity in cellular processes demonstrates its determining function in basic traits of cellular homeostasis, including growth, myotube formation and stress protection.

Recently, I was able to demonstrate the co-localization of isoforms ALDH1A1 and ALDH1A3 in SCs of human skeletal muscle tissue (Rihani et al., submitted data). Further, ALDH1 enzymatic activity has been identified as a hallmark of myoblast subpopulations with high myogenic capacity and increased resistance against oxidative stress (Vella et al., 2011). Most recently, Etienne et al., 2020, pointed out the important role of ALDH isoforms in muscle physiology and homeostasis, in particular in the context of healthy, aged and muscle-accentuated diseased muscle. Nevertheless, the functional role of ALDH1 isoforms in the process of myogenesis is demonstrated but not yet characterized in detail.

The present study should clarify the molecular mechanism of ALDH1A1 and ALDH1A3 isoforms in myogenesis including the processes of proliferation and differentiation in skeletal muscle. Furthermore, the effect of various treatments on ALDH1 isoforms and muscle cell behavior was addressed.

Satellite cell-like muscle cells were investigated using human (RH30, RD) and murine (C2C12) myoblast cell lines. The examination of different species encourages a comprehensive

conclusion about species-independent SC behavior and ALDH1 activity. All cell lines showed characteristic proliferation and terminal differentiation process.

Here, I could demonstrate a prevalent function of isoforms ALDH1A1 and ALDH1A3, respectively, in the process of myogenic differentiation. In detail, ALDH1A1 and ALDH1A3 proteins are essential for myotube formation. Findings could be confirmed using recombinant overexpression of ALDH1A1 and ALDH1A3 as well as genomic knockout of ALDH1A1 and ALDH1A3.

D. Material and Method

1. Primary and Secondary Antibodies, cDNA Clones

Table 1: Primary Antibodies

Antibody name	Company	Order-number	Clonality, Lot-number	Istotype	Reactivity	kDa	Dilution, Application
α-Actin	Santa Cruz	sc-58671	Monoclonal, J1917	IgG1 mouse	Mouse, Rat	43	1:500 IF
ALDH1a1	Abcam	ab52492	Monoclonal, EP1933Y, GR41450-29	IgG1 rabbit	Mouse, Human	54	1:500 IF, 1:1000 WB
ALDH1a1	Abcam	ab131068	Polyclonal, GR191385-3	IgG1 rabbit	Rat, Human	54	1:500 IF, 1:1000 WB
ALDH1a1 c.p.	Novus	NB110-55451	Monoclonal, EP1933Y, GR41450-6,	IgG rabbit	Human, mouse	54	1:500 IF
ALDH1a3	Abcam	ab129815	Polyclonal, GR3211979-3	IgG1 rabbit	Mouse, Human, Rat	56	1:500 IF, 1:1000 WB
ALDH1a3	Novus	NBP2-15339	Polyclonal	IgG1 rabbit	Mouse, Human, Rat	56	1:1000 WB
CD29	Abcam	Ab30388	Monoclonal, JB1B	IgG1 mouse	Human, Pig	88	1:500 IF, 1:1000 WB
CD31	Abcam	Ab28364	Polyclonal	IgG1 Rabbit	Mouse, Human, Pig		
CD45	Abcam	Ab10558	Polyclonal	IgG1 Rabbit	Mouse, Pig, Human, Rat		
CD56	Cell Marque	156R-98	Monoclonal, MRQ-42,	IgG1 Mouse	Mouse, Human, Rat		1:4 IHC

CD56/ NCAM1	Abcam	Ab9018	Monoclonal, RNL-1	IgG1 mouse	Mouse, Human, Rat	140	1:500 IF, 1:1000 WB
GFP XP	Cell signaling	2956S	Monoclonal, D5.1	IgG1 rabbit	Transfected GFP, YPF, CFP	Add. 27	1:1000 WB
M-Cadherin	Santa Cruz	Sc-374093	Monoclonal, C-6	IgG1, mouse	Human	120	1:500 IF, 1:500 WB
Myogenin	Sigma	SAB1410814	Polyclonal, 8322	IgG1 rabbit	Mouse, Human	25	1:500 IF, 1:500 WB
Myosin 4	Invitrogen	14-6503-82	Monoclonal MF20, 4301341	IgG1 mouse	Mouse, Human, Rat	220	1:1000 WB
Myosin-Fast	Sigma	M4276	Monoclonal, MY-32	IgG1 mouse	Mouse, Human, Rat	200	1:500 WB
PAX7	Abcam	Ab199010	Monoclonal, PAC7497	IgG1 mouse	Mouse, Rat, Human	57	1:500 IF, 1:1000 WB
Vinculin	Abcam	Ab129002	Polyclonal, GR221671-2	IgG1 rabbit	Mouse, Human, Rat	124	1:20.000 WB

Table 2: Secondary Antibodies

Antibody name	Company	Order- number	Lot-number	Dilution	Dye
Anti-Mouse IgG1 Magnetic Beads	Milentyi Biotec	130047102		10µl per 200µl	PE-label
Anti-Rabbit IgG1 Magnetic Beads	Milentyi Biotec	130048602		10µl per 200µl	PE-label
Donkey Anti-Rabbit	Thermo Fisher Scientific, Invitrogen	A10042	1366516	1:500	AlexaFluor 568 - red
Donkey Anti-Mouse	Thermo Fisher Scientific, Invitrogen	A10036	1272407	1:500	AlexaFluor 546 – red

Goat Anti-Rabbit (HRP-linked)	Abcam	ab721	GR3230320-2	1:5000	
Goat Anti-Mouse (HRP-linked)	Cell signaling	7076S	33	1:3000	
Hoechst 33342, Fluoro Pure Grade	Thermo Fisher Scientific	H21493		1:20000	Fluorescent blue
DAPI, Quenching Kit	Vector	SP-8500		Ready to use glue	Blue Fluorescent

Table 3: cDNA plasmidvector of ALDH1A1 and ALDH1A3

Substances	Catalog Number	Company
ALDH1a1 Mouse GFP-tagged ORF Clone	MG208039	Origene
ALDH1a3 Mouse GFP-tagged ORF Clone	MG222097	Origene

2. Cell Culture

2.1. Consumables and Additives

Table 4: Liquid Materials of Cell Cultivation

Substances	Catalog Number	Company
Dulbecco's Modified Eagle's Medium (DMEM) high-glucose without Pyruvate	41965062	Life Technologies
Dulbecco's Modified Eagle's Medium (DMEM) GlutaMAXX without Pyruvate	10566016	Life Technologies
Fetal Bovine Serum	10270106	Life Technologies

Ham's F10 Nutrient Mix	7340270	Life Technologies
HEPES	31550023	Sigma Aldrich
Minimum Essential Medium (MEM)	M2279	Sigma Aldrich
Phosphate Buffered Saline (PBS)	1 4190250	Thermo Fisher Scientific
Trypsin-EDTA	25200072	Life Technologies
µl-slides 8-well	80826	Ibidi

2.2. Cultivation and Cryopreservation of Cell lines

All cell lines were purchased at American Type Culture Collection (ATCC) and suitable for Biosafety Level 1. Cultivation Medium was used without Pyruvate additive. For proliferated cells 10% FBS was subsituted to high-glucose medium. For differentiation 2% Horse Serum in high-glucose medium was used. Passaging by 2 ml Trypsin after PBS washing, was performed three times a week depending on the confluence. After 3 minutes of Trypsin incubation, process could be blocked with an equal volume of medium. Cultivation was performed without antibiotics. Fresh flasks were uses every passage. Twice a year mycoplasma test was conducted with InVivo PlasmoTest.

For freezing of cell stocks a freezing medium containing 90% FBS and 10% DMSO was applied. Aliquots containing about 4 x 10^4 cells were stored overnight in -80°C and were put in liquid nitrogen for longtime storage.

2.3. Myogenic Cell lines

Myogenic cell lines C2C12, RH30 and RD were cultivated in serum-high standard medium for proliferative growth and are depicted in Figure 12. High confluence should to be avoided due to the possible induction of spontaneous myotube formation.

Controlled differentiation could be induced by serum-withdrawal (from 10% FBS to 2% Horse Serum) and is after 4 to 6 days' progress clearly visible by myotube formation. Macroscopic differentiation is depicted in Figure 13 and characterized by an elongated shape with a nearly parallel structuration.

Table 5: Cell lines

Name	Tissue	Organism/ Species	Cell Type/ Morphology	Culture Property	Disease
C2C12 (CRL-1772)	Muscle	Mus musculus, mouse	Myoblast	Adherent	
RD (CCL-136)	Muscle	Homos sapiens, human	Spindle cells and large multinucleated cells	Adherent	Embryonal Rhabdomyosarcoma
RH30 (CRL-2061)	Muscle	Homo sapiens, human	Fibroblast	Adherent	Alveolar Rhabdomyosarcoma

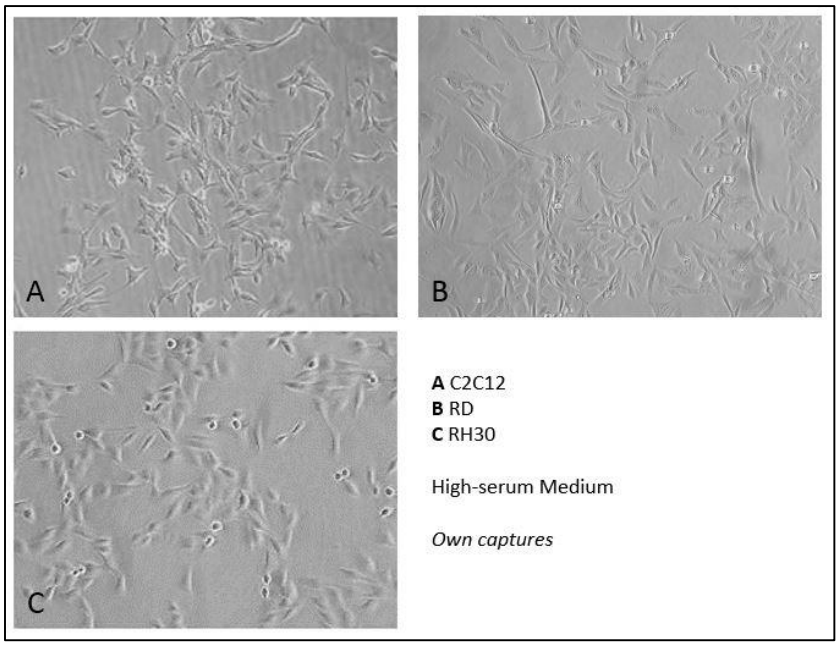

Figure 12: Exemplary cell line morphology in proliferation, 10x magnification

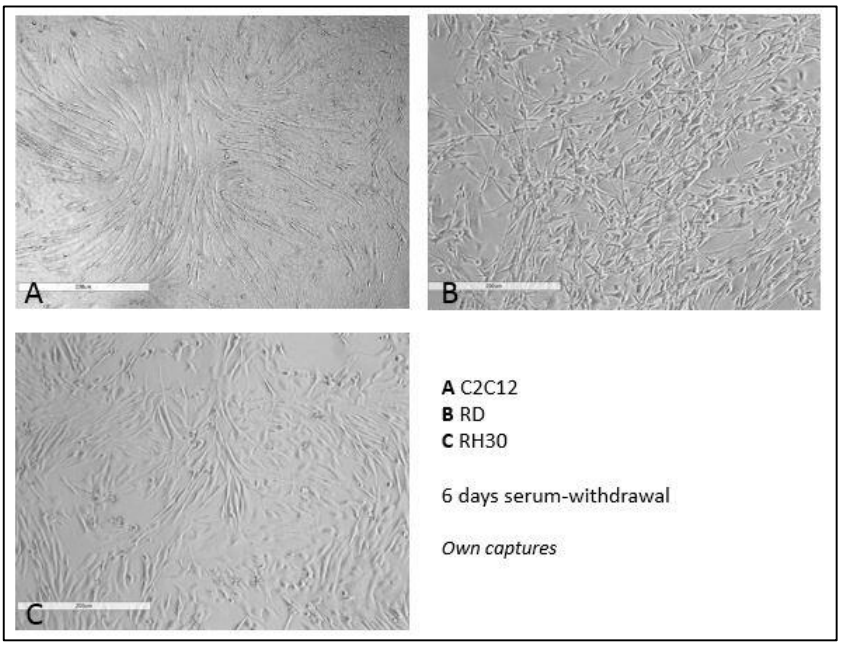

Figure 13: Exemplary cell line morphology of differentiated state A,C after 6 days, B after 8 days, 10x magnification

3. Western Blot Analysis

3.1. Sample Preparation

3.1.1. RIPA Buffer and Bradford Assay

For protein solubilization RIPA Buffer (radio immunoprecipitation assay) was prepared (Table 6) and was stored at -20°C Aliquots of 1 ml were substituted with 10 µl protease/ phosphatase inhibitor. For protein isolation 80 µl of RIPA-Buffer per 10^6 cells was added on PBS-washed cells, which were subsequently harvested with a cell scraper. The membranes were disrupted and the sample was collected. After subsequent sonication, the lysis was incubated for 15 minutes on ice. Lysis was pelleted (13.000 rpm for 10 minutes at 4°C) and the supernatant was collected.

The protein concentration was measured in triplets using Bradford assay (Table 7) and was read out with a microplate absorbance reader at a wavelength of 465 nm to 595 nm. The exact protein concentration was calculated using a BSA-protein standard curve with concentrations of 0.05, 0.1, 0.2, 0.4 and 0.8. Standard curve and samples were pipetted in triplets on a 96-well. Calculation was conducted in an Excel table.

Table 6: RIPA Buffer Stock Protocol

Reagent	Final concentration
SDS	0.1 %
Tris-Cl	10 mM
EDTA	0.5 mM
Triton X-100	1 %
NaCl	140 mM
Sodium deoxycholate	0.1 %

Table 7: Protocol for Bradford Assay

Component	Amount
Samples diluted to 1:10	4 µl sample + 36 µl ddH_20
Dye Reagent diluted to 1:5	200 µl total per sample

3.1.2. Protein Denaturation and Laemmli Buffer

For breaking up secondary and tertiary structures in the protein lysis Laemmli buffer with additional SDS and DTT was used. SDS (sodium dodecyl sulfate) is an anionic detergent, which is also coating proteins with negative charge for later electrophoresis. DTT (Dithiothreitol) is reducing disulfide bonds and stabilizes the lysate for freeze-thawing-cycles. Lysis and Laemmli was combined in a dilution of 1:5 and cooked for 5 minutes at 95°C and stored at -20°C. Gel running was performed in 1x Running Buffer diluted in ddH_20. For transfer 1x Transfer Buffer (1 l) contained 200 ml of 96% Ethanol and ddH_20. Washing buffer stock 10x TBS buffer was adjusted to a of pH 7.5 using HCl. For 1x TBS-T, 100 ml of 10 x TBS was diluted in ddH_20 and supplemented with 0.05 % Tween-20.

For blocking step, a 5 %Blocking Buffer with Roti-Block diluted in ddH_20 was used.

Table 8: 5x Laemmli Buffer Protocol

Reagent	Volume	Final concentration
SDS	1 g	2 %
1.5 M Tris-Cl (pH 6.8)	2.1 ml	63 mM
Gylcerol	5 ml	10 %
1 % Bromphenol blue	0.2 ml	0.004 %
H_20	2.7 ml	
Total	10 ml	

3.1.3. Western Blot Buffer

Table 9: 10x Running Buffer ingredients

Reagent	Volume	Final concentration
Tris	30.3 g	0.25 M
Gylcine	144.1 g	2 M
SDS	10 g	1 %
Total	1 l	

Table 10: 10x Transfer Buffer Ingredients

Reagent	Volume	Final concentration
Tris	30.3 g	0.25 M
Glycine	142.6 g	2 M
Total	1 l	

Table 11: 10x TBS Buffer Ingredients

Reagent	Volume	Final concentration
Tris	24.2 g	0.2 M
NaCl	87.66 g	1.5 M
Total	1 l	

Table 12: Stripping Buffer Ingredients

Reagent	Volume	Final concentration
Tris (pH 6.8)	12.5 ml	0.5 M
ddH_20	67.5 ml	
10 % SDS	20 ml	
2-mercaptoethanol	0.8 ml	

Total	100.8 ml

3.2. Gel Preparation Protocols

Depending on the molecular weight of desired proteins, the separation gel should be selected. For proteins up to 50 kDa 12 % gels, over 50 kDa to 200 kDa 8 % were best. 10 % gel was used for detection of both small and big size proteins.

Table 13: Separation Gel Protocol

Components	**8 %**	**10 %**	**12 %**
H_20	6.9 ml	5.9 ml	4.9 ml
30 % Acrylamide	4.0 ml	5 ml	6 ml
1.5 M Tris (pH 8.8)	3.8 ml	3.8 ml	3.8 ml
10 % SDS	150 µl	150 µl	150 µl
10 % APS	150 µl	150 µl	150 µl
Temed	9 µl	6 µl	6 µl

Table 14: Stacking Gel Protocol

Gel percentage	5 %
Components	
H_20	5.5 ml
30 % Acrylamide	1.3 ml
1.5 M Tris (pH 6.8)	1.0 ml
10 % SDS	80 µl
10 % APS	80 µl
Temed	8 µl

3.3. Western Blot Procedure

Lysis was loaded onto prepared SDS-gels for protein. Protein concentration was determined before by Bradford assay, as described in 3.1.1 and the calculated amount of 25 mg protein was loaded in each lane. With a Voltage of 160 the separation took about 50 minutes. Afterwards gel with separated protein was put together with a methanol-activated PVDF-membrane for transferring protein onto the membrane with a Wet Blot procedure at 110 V for 60 minutes. For transfer-control Ponceau-Red staining visualized protein lanes on the membrane. Blocking with 5 % Blocking Buffer for 60 minutes at room temperature prevented unspecific binding of the later applied primary antibody. Primary antibody was added to Blocking Buffer and the membrane was incubated overnight at 4°C gently mixing. Washing several times with TBS-T was performed for removing primary antibody residual. Next, membranes were incubated at room temperature in Blocking Buffer for 45 minutes with HRP-linked secondary antibody, which was specific for the species of the first antibody. Afterwards membrane was again washed with TBS-T several times. For the visualization of protein bands HRP-substrate (Cell signaling) for chemiluminescence detection was used.

4. Aldefluor Assay

Fluorescent Aldefluor reagent system (StemCell Company) was used for the measurement of ALDH enzyme activity in flow cytometry. The uncharged substrate BAAA (BODIPY-aminoacetaldehyde) diffused passively into living cells by uptake through ALDH, converted BAAA into BAA (BODIPY-aminoacetate), which then activated fluorophore Aldefluor. BAA was negatively charged and retained inside the cell due to efflux inhibitors Verapamil and Fumitremorgin C. BAA accumulation representws ALDH enzyme activity of measured cells and was detected by accumulation of green fluorescent dye. Only viable cells were illustrated because dead cells loosed BAA through broken membranes. Flow cytometry analysis was

conducted in combination with an ALDH inhibited control (wildtype cells with DEAB) as blank. After adjustment by control measurement test samples could be examined.

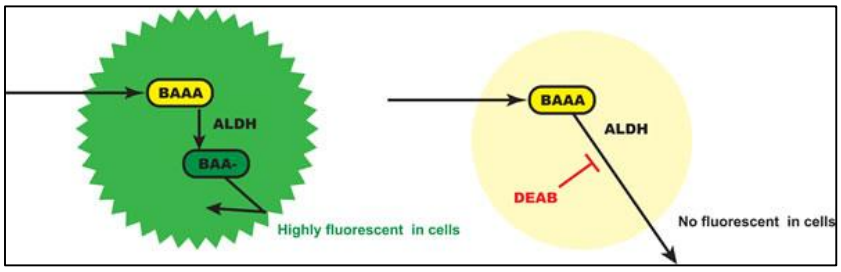

Figure 14 Analysis: of BAAA metabolism in Aldefluor Assay (from Tomita et al., 2016)

Table 15: Aldefluor Assay Protocol

	Component	**Amount**
Mixture I (test)	DMEM w/o FBS	1 ml
	Verapamil	1 µl
	Fumitremorgin C	1 µl
Mixture II (control)	DEAB (1.5 mM in 95 % Ethanol)	15 µl
	Add half of Mixture I to II	

For preparation 500.000 cells were trypsinized, washed with PBS and added into Mixture I with freshly supplemented 5 µl of undiluted Aldefluor reagent. 500 µl of Mixture I-cell-suspension was immediately transferred into Mixture II for ALDH enzyme inhibition as negative control sample. Both groups were incubated for 30 minutes at 37 °C in the dark. Cells were then pelleted and stored on ice until measurement. Supernatant was aspirated for further pellet preparation. Samples were resuspended in Aldefluor Assay Buffer directly before analysis. Floy Cytometer was adjusted with negative control. Next, the corresponding samples was measured. Gathered raw data was analyzed using FlowJo program, where in Quarter 2 (Q2) positive cells were illustrated in percentage. In Figure 15 an example of C2C12

wildtype (WT) cells is depicted. On the left side the DEAB-inhibited and therefore, negative sample was adjusted to 0 % enzyme activity. Positive sample here demonstrated an activity of over 40 % (Q2).

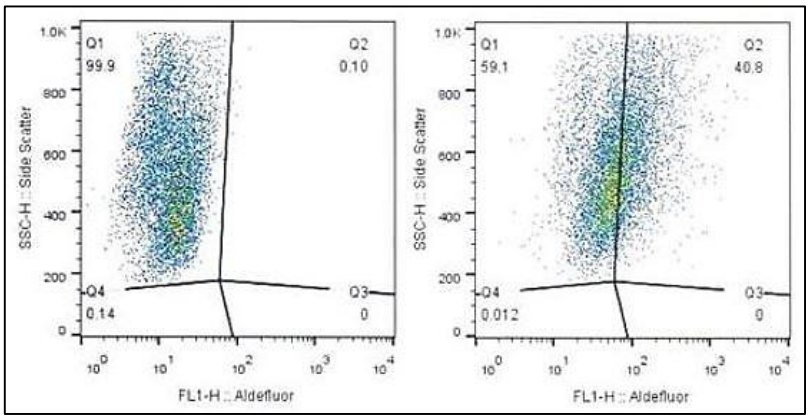

Figure 15: Example of FlowJo Aldefluor Assay analysis in WT C2C12 cells (left control, right test sample)

5. Immunofluorescence of Fixed Cultured Cells

Myoblast cell lines were seeded in an amount of 4 x 10^4 per well on an 8-chamber cover slide and cultivated in 400 µl medium overnight. On the next day treatment with either serum-withdrawal or DSF-treatment began. The chambers could be removed from the slide after treatment and cells could be fixated.

For immunofluorescent staining slides was prepared. Treated cells were washed with PBS and fixed with 4 % formaldehyde for 15 minutes and washed twice with PBS. Cells were incubated for 20 minutes at room temperature with Blocking Buffer (Figure 15) with additional serum depending on secondary antibody. After washing once with PBS primary antibody diluted in Blocking Buffer is added and incubated over night at 4 °C. On the next day cells were washed once with PBS and incubated for 20 minutes at room temperature in the dark with secondary antibody conjugated with fluorescent proteins. Secondary antibody was diluted in Blocking Buffer. Washed cells were then incubated for 10 minutes at room

temperature in the dark in DAPI (4′ ,6-Diamidin-2-phenylindol) diluted in H_20 for nucleic staining. Slides were mounted and consecutively analyzed with a fluorescence microscope. Immunofluorescence could be preserved for a longer time when stored in dark at 4 °C.

Table 16: Blocking Buffer Stock Protocol

Component	Amount	Final Concentration
PBS	500 ml	1x
BSA	5 g	1 %
TX 100	0.5 ml	0.1 %
Gold Fish Gelatine	1 g	0.2 %
Natrium Azid	1 ml of 10 % stock	0.02 %
Donkey Serum	Add at usage	2.5 %

6. CRISPR/Cas9 Editing

6.1. Single Guide RNA Design

Online-tool from research lab at MIT (Massachusetts Institute of Technology) was used for oligo design (https://zlab.bio/guide-design-resources, 5th 07 2020) and single guide RNA (sgRNA) and was conducted as in Wu et al., 2018. Oligos were then BLASTed (Basic Local Alignment Search Tool) again for specifity.

Table 17: sgRNA: Oligonucleotides for CRISPR/Cas 9 Knockout

Oligos	Sequences (5’ -> 3’)
human	
ALDH1a1_gRNA_01_forward_human	CACCGAATCTTCAAATCGGTGAGT
ALDH1a1_gRNA_01_reverse_human	AAACACTCACCGATTTGAAGATTC
ALDH1a3_gRNA_01_forward_human	CACCTTCCACGGCCCCGTTAGCGG

ALDH1a3_gRNA_01_reverse_human	AAACCCGCTAACGGGGCCGTGGAA
mouse	
ALDH1a1_gRNA_01_forward_mouse	CACCGCATACTTGTCGGATTTAGGAGG
ALDH1a1_gRNA_01_reverse_mouse	AAACCCTCCTAAATCCGACAAGTATGC
ALDH1a3_gRNA_01_forward_mouse	CACCTTGACCTCCAAGTTGCGGATGGG
ALDH1a3_gRNA_01_reverse_mouse	AAACCCCATCCGCAACTTGGAGGTCAA

6.2. sgRNA Oligos Inserts

The oligos were suspended to a final concentration of 100 µM with sterile water and annealed. The annealing mixture and annealing temperature is indicated in the following table.

Table 18: Annealing mixture for sgRNA oligos

Component	Amount (µl)
T4 PNK	1
T4 ligation buffer	1
sgRNA forward (100µM)	1
sgRNA reverse (100µM)	1
ddH_20	6
Total volume	10

The oligos were consecutively phosphorylated and annealed at 37 °C for 30 minutes with following 95 °C for 5 minutes and ramping down to 25 °C at 5 °C/ minute. After annealing, the oligos were diluted to 1:200 in sterile water and stored at -20 °C.

6.3. Linearization of pSpCas9 Plasmid DNA

The plasmid pSpCas9(BB)-2A-GFP (PX458) was gifted by Feng Zhang (Addgene plasmid #48138; http://n2t.net/addgene:48138, 5th 07 2020; RRID: Addgene_48138) (Figure 16). The plasmid included a GFP-tag and the gRNA scaffold was located between the U6 promotor and the CMV enhancer, where restrictions digest cut and the sequence of interest was inserted by ligation. Inserted sequence depicted the Cas9 labeled sequence for genomic knockout.

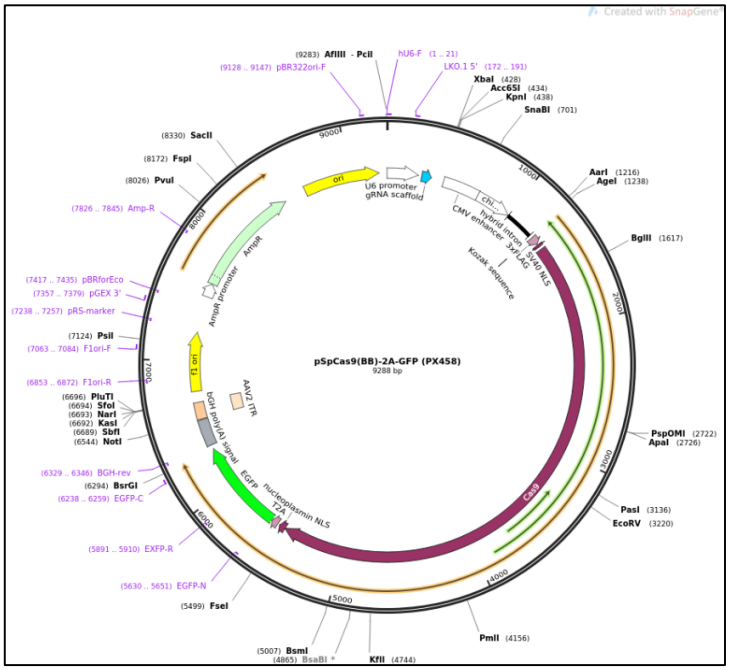

Figure 16: pSpCas9-2A-GFP (PX458) plasmid with cloning backbone for sgRNA (from http://www.addgene.org/48138, 5th 07 2020)

The following reagents (Table 19) were used for cutting the pSpCas9 plasmid into linearized DNA by incubation at 37 °C for 4 hours. Afterwards cutting was heat-inactivated at 65 °C for 20 min. Linearized plasmid was stored at -20 °C.

Table 19: Transformation Reagent Protocol

Component	Amount
DNA	8 µg
Restriction Enzyme BbsI	2.5 µl
NEB Buffer 2	5 µl
ddH_20	40.5 µl
Total	50 µl

6.4. Linear DNA Purification

A 0.6 % agar gel was used for linear plasmid separation and was running for 2 hours with 80 V. Circular pSpCas9 DNA plasmid was applied as size control.

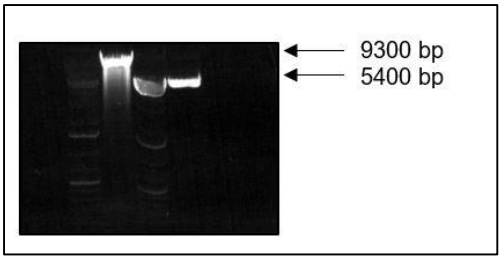

Figure 17: Exemplary electrophoresis: left to right: ladder, cut plasmid, ladder, non-cut plasmid

Successfully linearized plasmid depicted a longer product than non-cut plasmid. Linearized plasmid product was cut out of the gel and purified using QIAquick® Gel Extraction Kit. Briefly, the gel piece was sliced and dissolved in Buffer QG and mixed with isopropanol. The samples was then transferred through a QIAquick spin column. Purified DNA was eluted with 50 µl RNase-free water and its concentration was measured using a spectrophotometer (NanoDrop™ 2000c).

6.5. Ligation of sgRNA Oligos Inserts and pSpCas9 Linear DNA

The oligo inserts of sgRNA were prepared in 1:200 dilutions and stored at -20 °C. For the ligation of gRNA oligos and linearized plasmid the following mixture was incubated for 30 minutes at 16 °C.

Table 20: Protocol for Ligation of DNA and oligo inserts

Component	Amount (µl)
Linearized DNA	0.5; at least 50ng
gRNA oligo inserts	2
Solution I	2.5
Total	5

6.6. Transformation

Ligation mixture described in 6.5 was used for consecutive transformation with NEB 5-alpha competent E. coli cells. 5 µl of the ligation was pipetted into freshly thawed E. coli aliquots, incubated for 30 min on ice and subsequently heat-shocked at 42 °C for 30 seconds. After 5 minutes of incubation time on ice, the bacteria were incubated for 60 minutes at 37 °C with 950 µl SOC medium on a shaker. Pelleted bacteria with a residual of 1 ml SOC medium were resuspended in fresh SOC medium and applied on a selective agar plate supplemented with Ampicillin. For amplification control one agar plate was with non-transformed E. coli and without Ampicillin supplement. Plates were incubated overnight at 37 °C.

6.7. Single Clone Picking and PCR

Eight clones per agar plate were picked and tested for specificity. Clones were amplified by PCR using forward primer sequence of U6 promotor and reverse primer of 5' to 3' sequence of gRNA sequence of interest. The washed out template of the picked clones was at the same time on a shaker with outgrowth medium.

U6 forward primer sequence was: GAGGGCCTATTTCCCATGATTCC. For PCR the following program was used (Table 21).

Table 21: Single Clone PCR Protocol

Step	Temperature	Duration
Initial denaturalization	95°C	30 seconds
Amplification with 30 cycles	95°C	30 seconds
	58°C	1 minute
	68°C	30 seconds
Final Extension	68°C	5 minutes
Hold	10°C	

PCR products were loaded onto a 2 % gel and electrophoresis was performed for 30 minutes supplied with 100 V. Successful cloning was indicated by a 100 to 200 bp size. Positive bands were noted down and corresponding medium stocks with outgrown ligation plasmids were subsequently amplified overnight at 37 °C with 130 rpm using a maxi stock of LB medium supplemented with Ampicillin (100 µg/ ml).

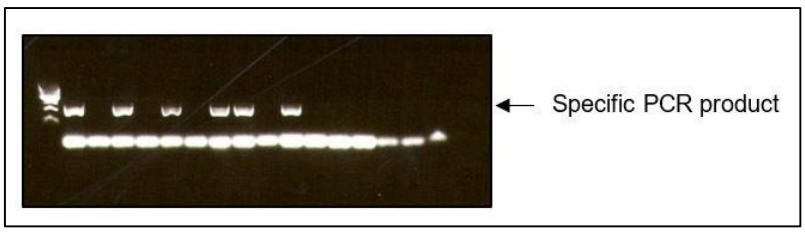

Figure 18: Electrophoresis result of exemplary human sgRNA ALDH1A1 clones

6.8. Plasmid Isolation and Sequencing

After overnight shaking half of the stock was frozen in 50 % glycerol at -80 °C for storage. With the second part plasmid isolation was performed using QIAprep spin miniprep Kit. Eluted DNA concentration was measured using NanoDrop 200c. The extracted plasmid was send in for sequencing using forward primer of U6 promotor sequence. The result was then blasted with the RNA sequence of interest for target specifity.

6.9. Cell Transfection and Cell Sorting

Human RH30 cells and mouse-derived C2C12 cells were plated in 10cm Dishes, each with 500.000 cells and attached overnight. Cells were consecutively transfected on the next day using plasmids with ALDH1A1 and ALDH1A3, respectively, insert and lipofectamine 3000.

Per 10cm Dish following mixture was applied:

Table 22: Transfection with Lipofectamine 3000 Protocol

	Component	**Amount per sample (µl)**
Mixture I	Opti-MEM Medium	250
	Lipofectamine 3000	15
Mixture II	Opti-MEM Medium	250
	DNA	XX µl equal to 10 ng
	P3000 Reagent	10

For preparation mixture I and II were combined and incubated for 5 minutes at room temperature and applied on cultivated cells. As transfection control empty GFP vector was transfected in a separate group of cultured cells. 48 hours post transfection, the cells were

analyzed by microscopy and fluorescence filter for GFP signal and transfection-efficiency was documented.

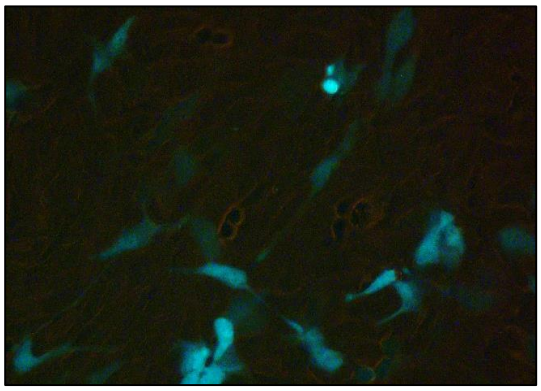

Figure 19: Example of transfected, non-sorted C2C12 cells with pSpCas9-ALDH1A3 plasmid, x20 magnification

Then the transfected cells were trypsinized and pelleted. Samples were resuspended in sorting buffer (3% FBS, 1mM EDTA in PBS) and filtered through a single cell filter. Succesfully transfected cells were sorted by GFP-signal using a fluorescence activated cell sorter (FACS ARIA III) and laser for FITC wavelength (561 nm).

For adjustment of the sorting machine Forward- and Sideward-Scatter (FSC, SSC) was adjusted with non-transfected and unstained control. The blue population in Figure 20 depicts vital FITC-negative wildtype cells and were used for gating.

After adjustment the sorter detected GFP-positive cells in the inhomogeneous sample and sorted them into a new tube with pure FBS. FITC-cells are demonstrated in the area of p4, which are in Figure 21 depicted in green.

After sorting GFP-positive cells were plated in a fresh dish. After 2 weeks a knockout (KO) validation was performed using protein analysis in Western Blotting.

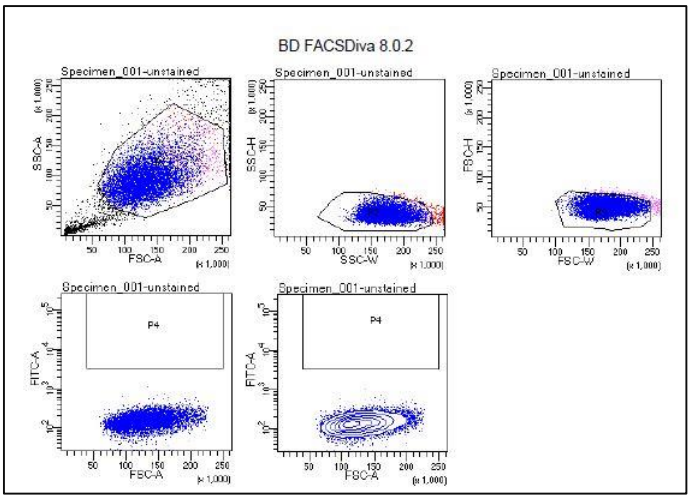

Figure 20: Adjustment of ARIA III sorter for exemplary unstained wildtype C2C12 cells

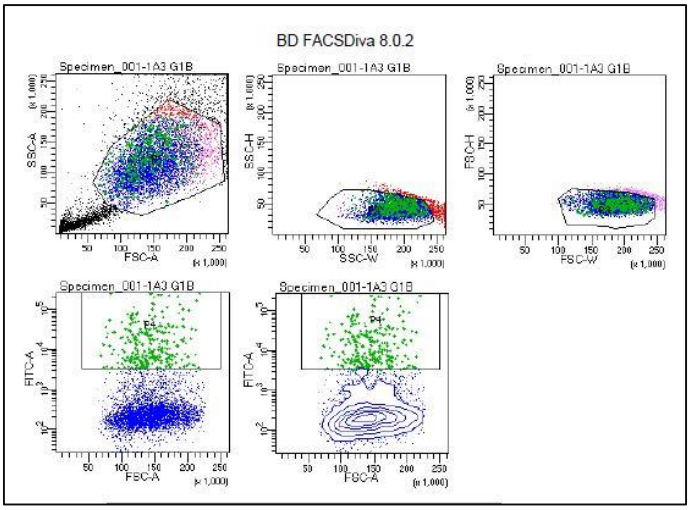

Figure 21: Example of sorted C2C12 cells transfected with pSpCas9-ALDH1a3plasmid

7. Recombinant ALDH1a1 and ALDH1a3 Overexpression

For specific ALDH1 isoform overexpression a pCMV6 vector with an open reading frame (ORF) including Turbo Green Fluorescent Protein (tGFP) on the C-terminus was applied. tGFP expression was used for successful transfection control. Two different ORF vectors were purchased: ALDH1A1 and ALDH1A3.

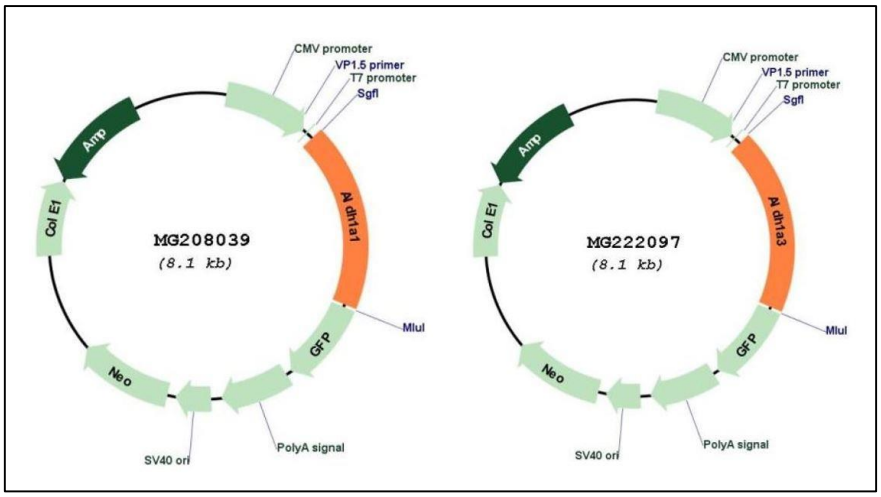

Figure 22: cDNA Clones of ALDH1a1- and ALDH1a3-GFP-tag

Ampicillin (Amp) resistance gene insert on the opposite strand was used for controlled expansion of the plasmid after competent cell amplification. Ampicillin was applied in a concentration of 100 µg/ml.

Transfection of 10^6 cells in 6 cm dishes was performed with Lipofectamine 3000 and Opti-MEM-Medium with (Table 23).

Table 23: Transient Transfection Buffer Protocol with Lipofectamine 3000

	Component	**Amount (µl) per sample**
Mixture I	Opti-MEM Medium	250
	Lipofectamine 3000	15
Mixture II	Opti-MEM Medium	250
	DNA	1,5 to 3 µg
	P3000 Reagent	10

GFP signal verified successful transfection of plasmids for a period of 24 - 48h upon transfection.

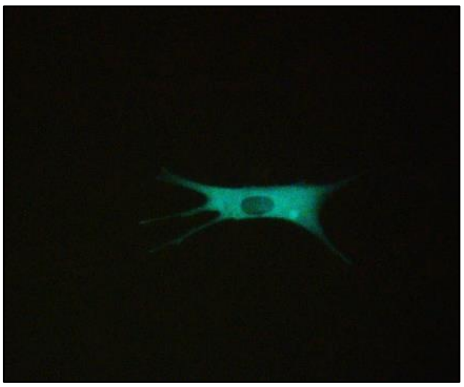

Figure 23: Capture of ALDH1A1 vector transfected C2C12 cell (magnification: 40x)

Neomycin-resistance was used for G418-/ Geneticin-selection and enabled stable transfection. G418 was applied in a concentration of 200 to 800 mg/ ml medium for 7 days and subsequently with 200 mg/ ml in medium. For Western Analysis antibodies against transfected ALDH1 isoform sequences and empty GFP vector was apllied.

E. Results

1. Adaptive Morphology by ALDH Inhibition

In proliferative status C2C12 and RH30 cells showed a typically roundish shape with small protrusions. Under conditions of serum-withdrawal differentiation (Diff) could be induced, depicting myotube formation with fused nuclei and an elongated, parallel co-located morphology. C2C12 demonstrated the highest proliferation turnover, followed by RH30. RD depicted a relatively slow turnover and was therefore, differing from other cell. Furthermore, RD cell differentiation was prolonged for two days in order to reach similar myotube formation status as seen in C2C12 and RH30 (Figure 13). Hence, RD cells were not directly comparable to C2C12 and RH30 growth behavior.

Growth behavior of cell lines C2C12, RH30 and RD was consecutively analyzed in conditions of enzymatic ALDH inhibition using chemical inhibitor Disulfiram (DSF). Consecutive 6 day DSF treatment evoked a differentiated morphology in C2C12 and RH30. RD cells were demonstrating clear morphological changes after additional 2 days of treatment. Non-treated control cells are labeled as Ctrl. (Figure 24)

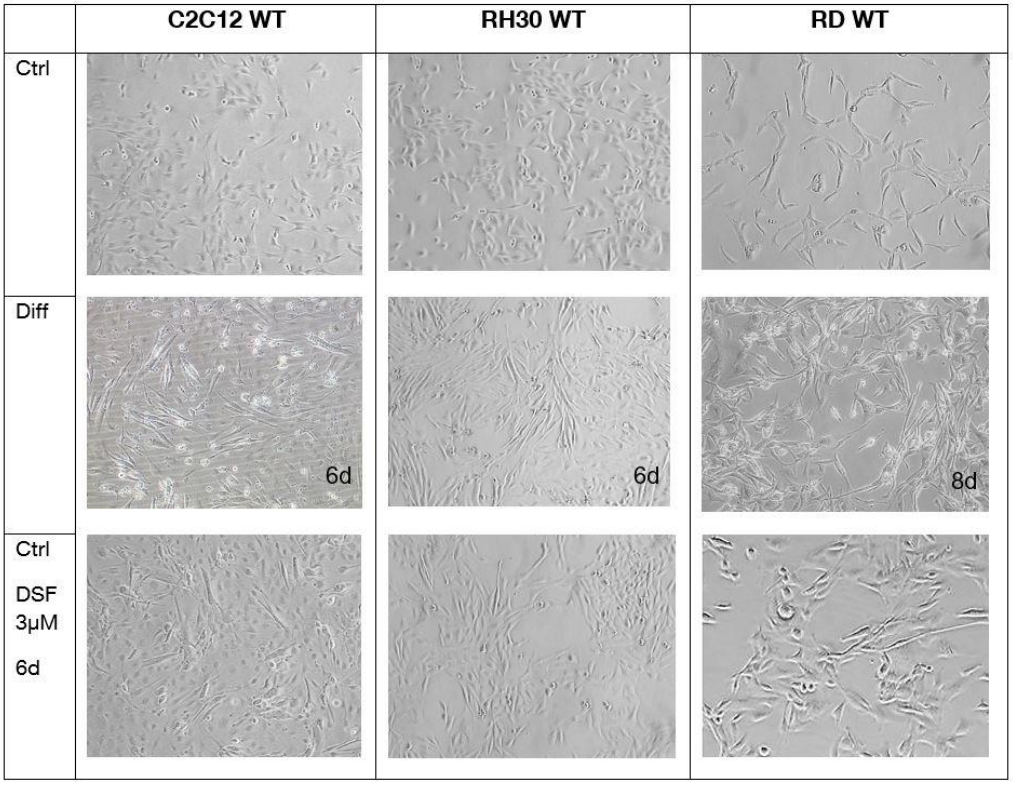

Figure 24: Capture of wildtype C2C12 and RH30 cells in different states (magnification: 10x,20x)

2. Protein Analysis

Samples of proliferation (Ctrl), differentiation (Diff) and DSF-treatment (DSF) were subsequently analyzed in Western Blot using antibodies against myogenic differentiation markers MF20 (220 kDa) and MHC (200 kDa) as well as against isoforms ALDH1A1 (54 kDa) and ALDH1A3 (56 kDa).

Differentiation process could be proved in all Diff samples. Ctrl of C2C12 and RH30 were not depicting a band specific for differentiation. However, RD Ctrl depicted protein levels of MF20 (Figure 26).

ALDH1A1 protein was not observed in C2C12 and RH30 Ctrl, whereas in RD Ctrl ALDH1A1 protein could be detected. Upon differentiation isoform ALDH1A1 protein demonstrated high levels in all Diff samples (Figure 25).

Evaluation of anti-ALDH1A3 antibody (Figure 25) showed in C2C12 Ctrl ALDH1A3, whereas in RH30 Ctrl low levels. Elevated levels of ALDH1A3 could be observed in Diff samples of C2C12 and RH30. Though, all samples of RD were negative for ALDH1A3 protein, only positive control LN229 depicted an ALDH1A3 specific protein band.

Consecutives analysis of DSF-treated samples revealed in C2C12 and RH30 high protein levels of ALDH1A1 and ALDH1A3 similar to Diff. In DSF treated RD sample protein level seemed to be not increased. Further analysis of DSF samples using myogenic differentiation marker revealed a positive band in all cell lines, indicating differentiation process. (Figure 26).

Altogether, in C2C12 and RH30 Diff samples and DSF-treated cells demonstrated high ALDH1A1 and ALDH1A3 protein levels. Furthermore, differentiation process was additionally proven in Diff samples and DSF. (Figure 25).

C2C12 and RH30 depicted reliable model system for the investigation of myogenic proliferation and differentiation. RD cells were excluded from further experiments, since they were negative for ALDH1A3 and demonstrated weak growth behavior.

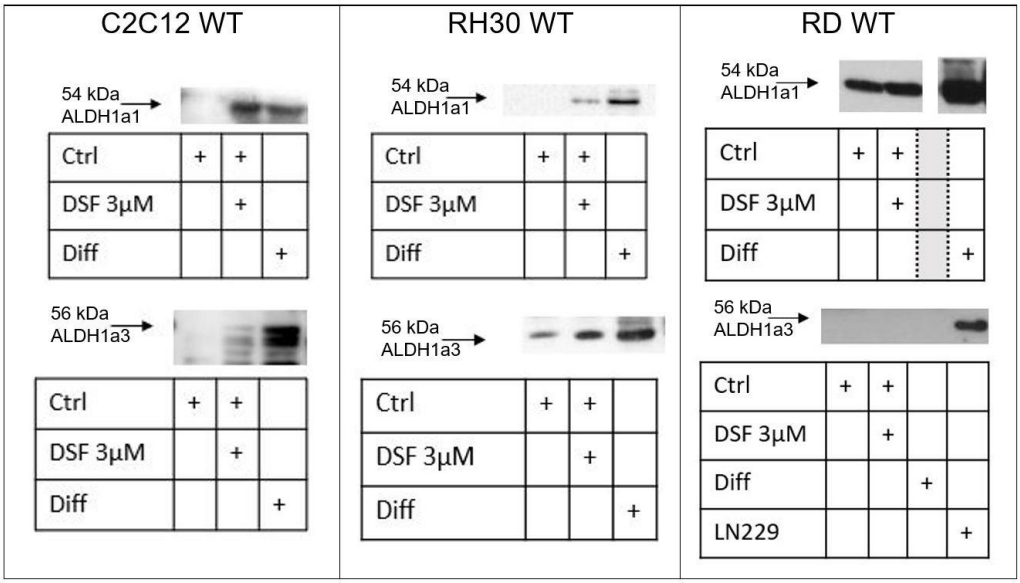

Figure 25: Western Blot of C2C12, RH30 and RD wildtype against ALDH1A1 and ALDH1A3

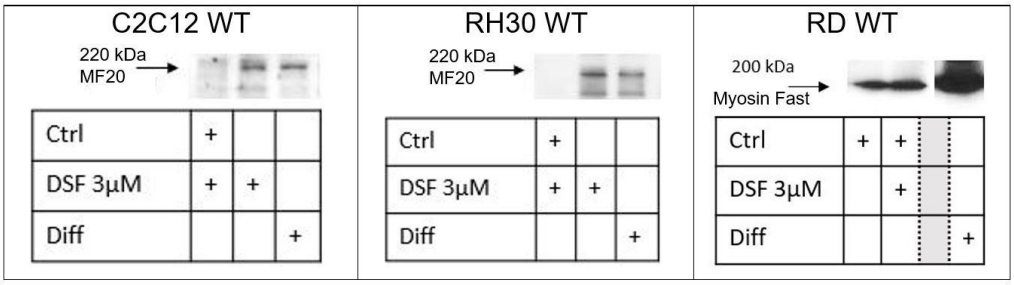

Figure 26: Western Blot of C2C12, RH30 and RD wildtype against MF20 and Myosin Fast

3. Enzymatic ALDH1 Activity in Differentiation

Enzymatic ALDH1 activity was measured in RH30 and C212 cells using Aldefluor Assay. Since chemical ALDH inhibitor DEAB is used for the negative control, DSF treated samples would not show any difference, therefore, only Ctrl and Diff samples were analyzed.

C2C12 Ctrl demonstrated an enzymatic ALDH1 activity level of 54.5 %, C2C12 Diff described an accumulation of 31.8 % with in total 86.3 % of ALDH1 activity.

RH30 wildtype cells showed in proliferating cells 28.0 % ALDH1 enzyme activity and in Diff 71.7 %, which resulted in an activity accumulation of 43.7 % upon differentiation.

The uptake of ALDH1 activity from Ctrl to Diff was observed to be higher in RH30 cell line.

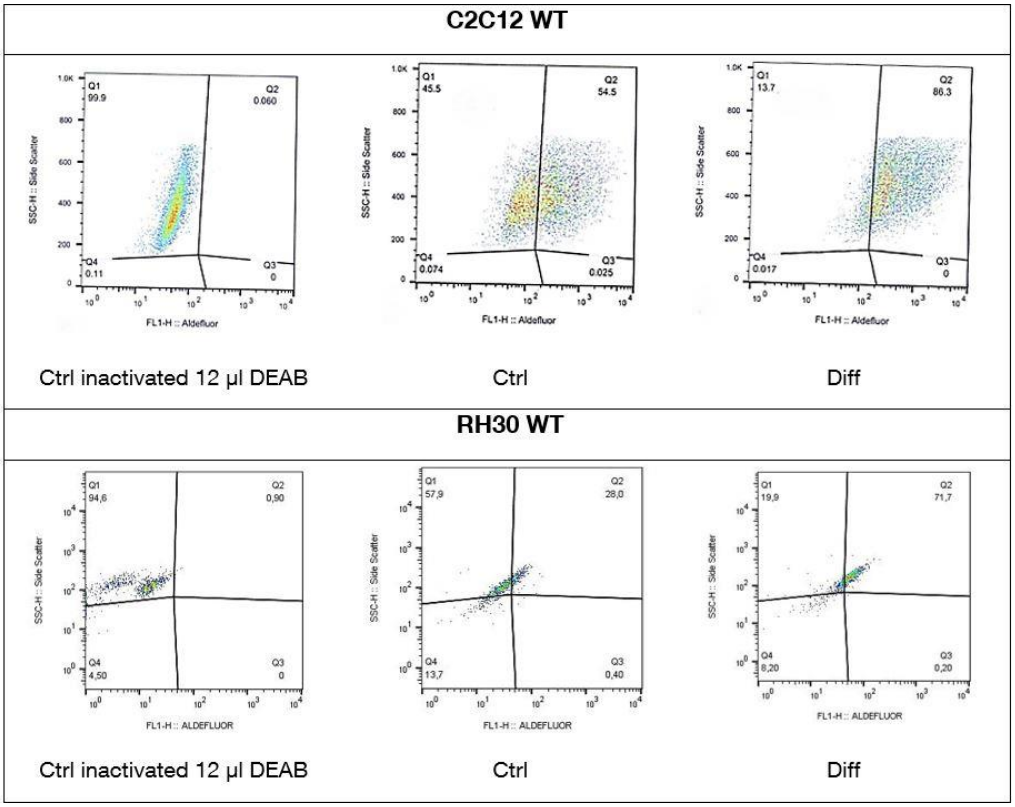

Figure 27: Aldelfuor Assay of C2C12 and RH30 Ctrl and Diff, ALDH1 activity is displayed with a shift into Q2

4. Immunofluorescent Staining

Using chamber-slides for cell cultivation and consecutive treatments indirect immunofluorescence (IF) was conducted using antibodies directed against the isoforms ALDH1A1, ALDH1A3 and differentiation marker α-Aktin.

In C2C12 Ctrl anti-ALDH1A1 and anti-ALDH1A3 antibody immunoreaction was low, whereas in Diff as well as in DSF-treated sample a higher expression could be observed (Figure 28).

Differentiation marker α-Aktin demonstrated low levels in C2C12 Ctrl and was found to be elevated in C2C12 Diff. DSF-treated C2C12 depicted a similar immunofluorescent staining pattern as observed in Diff (Figure 28).

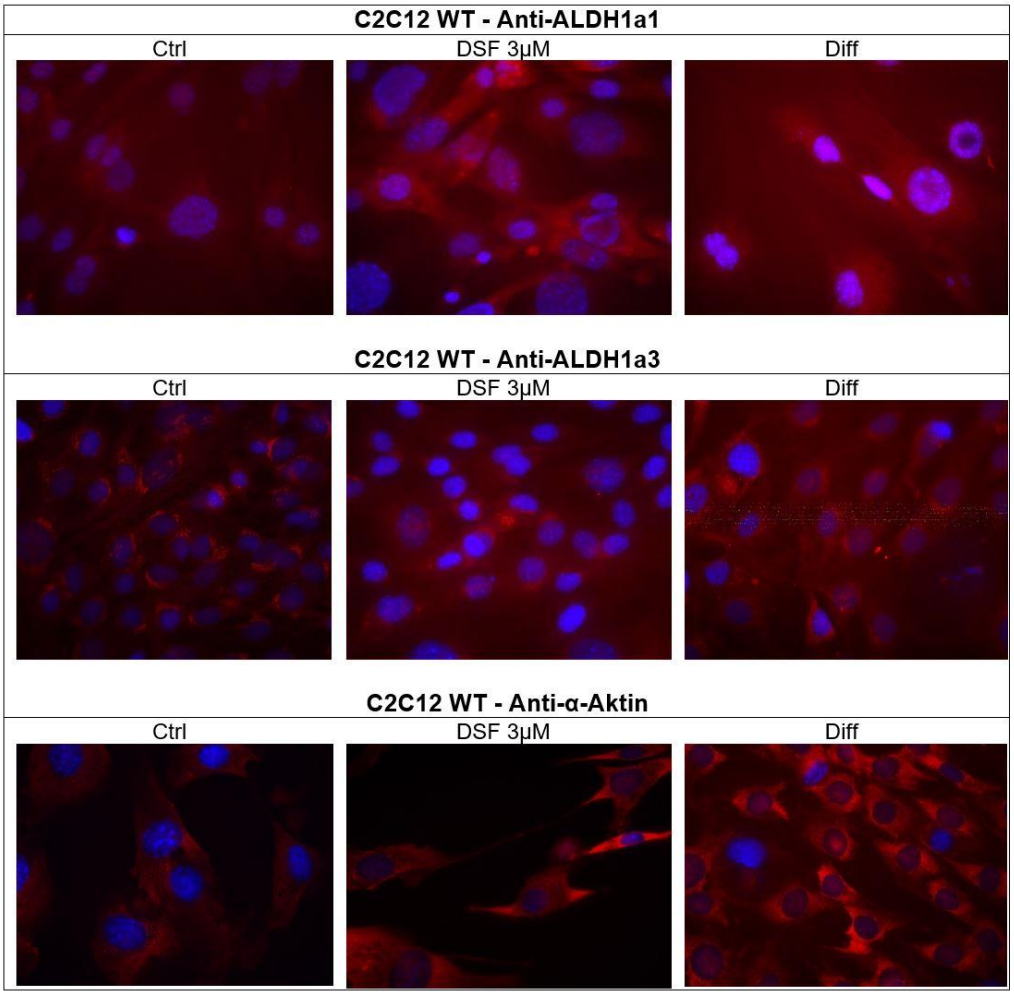

Figure 28: Immunofluorescent staining against ALDH1A1, ALDH1A3 and α-Aktin with C2C12 wildtype

RH30 showed a comparable expression pattern (Figure 29). Anti-ALDH1A1 and anti-ALDH1A3 antibody immunoreaction in RH30 Ctrl was low in comparison to increased levels of Diff samples.

DSF-treated RH30 cells expressed ALDH1A1 and ALDH1A3 in a comparable intensity of differentiated RH30.

Antibody reaction to α-Aktin was found to be low in RH30 control, whereas Diff and DSF-treated RH30 illustrated a strong positivity.

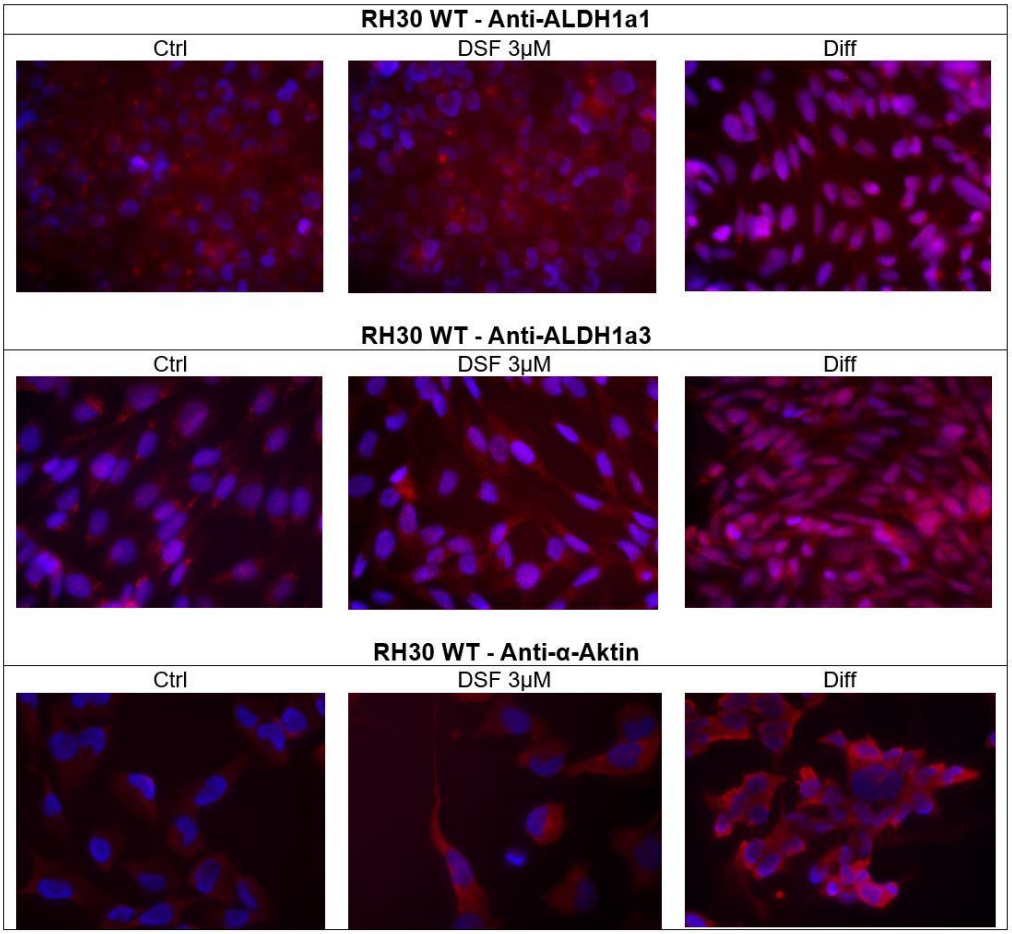

Figure 29: Immunofluorescent staining against ALDH1A1, ALDH1A3 and α-Aktin with RH30 wildtype

Both, C2C12 and RH30, showed an increased expression to antibodies of ALDH1A1 and ALDH1A3 upon differentiation status. Differentiation was indicated in Diff and DSF-treatment samples.

5. Recombinant Overexpression of ALDH1 Isoforms in C2C12 Cells

For the examination of myogenic growth behavior in conditions of ALDH1 isoform overexpression, stable transfection of plasmidvectors with recombinant ALDH1A1 and ALDH1A3, respectively, insert was performed.

Successfully transfected cells depicted green fluorescence GFP, which could be observed for about 48h upon transfection. Referring to the illustrated GFP-signal pattern ALDH1A1 plasmidvector transfection depicted a higher transfection efficiency than ALDH1A3 (Figure 30).

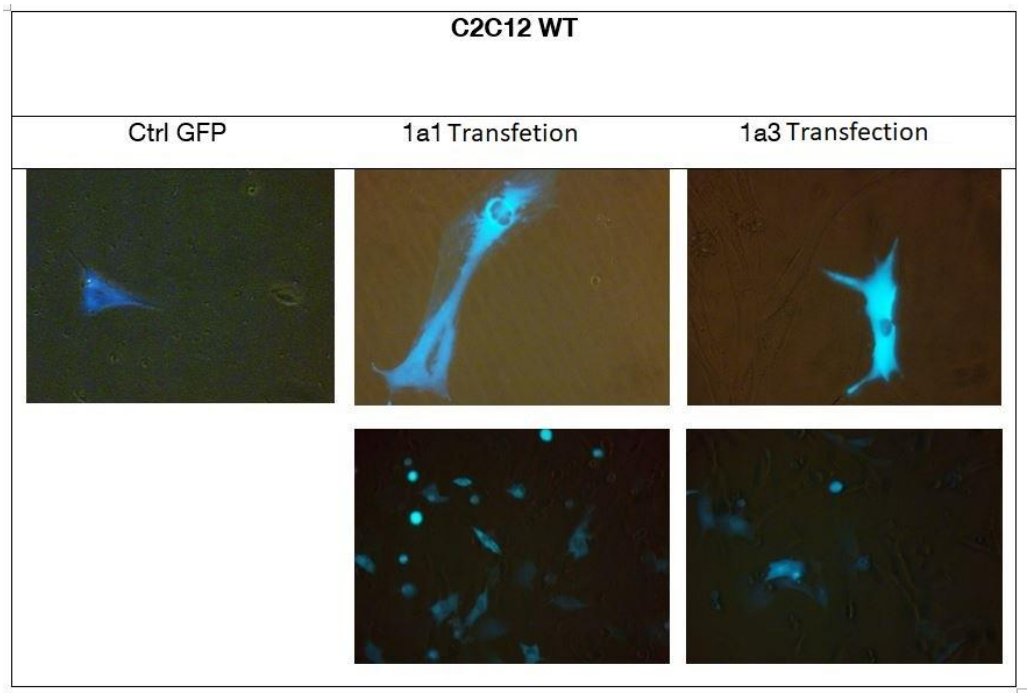

Figure 30: Capture of C2C12 cells transfected with GFP, C2C12 transfected with plasmidvector of ALDH1 isoforms ALDH1A1 and ALDH1A3 including GFP-tag (magnification: 20x and 40x)

Since transfected cells were resistant to Neomycin, cells were consecutively purified with G418-treatment upon two days post transfection.

Figure 31 depicts the morphological change of transfected cells after 7 days of G418-selection. ALDH1A1 and ALDH1A3, respectively, overexpressing C2C12 cells (1a1 V, 1a3 V) demonstrated an elongated shape, resembling myotube formation.

Samples of C2C12 control with and without GFP showed typical proliferation behavior, whereas G418-treatment induced apoptotic behavior in C2C12 Ctrl. Since exemplary GFP-transfection did demonstrate morphological changes and G418-treatment in Ctrl lead to apoptosis due to lacking resistance, both treatments are evidently not inducing adaptive cell behavior.

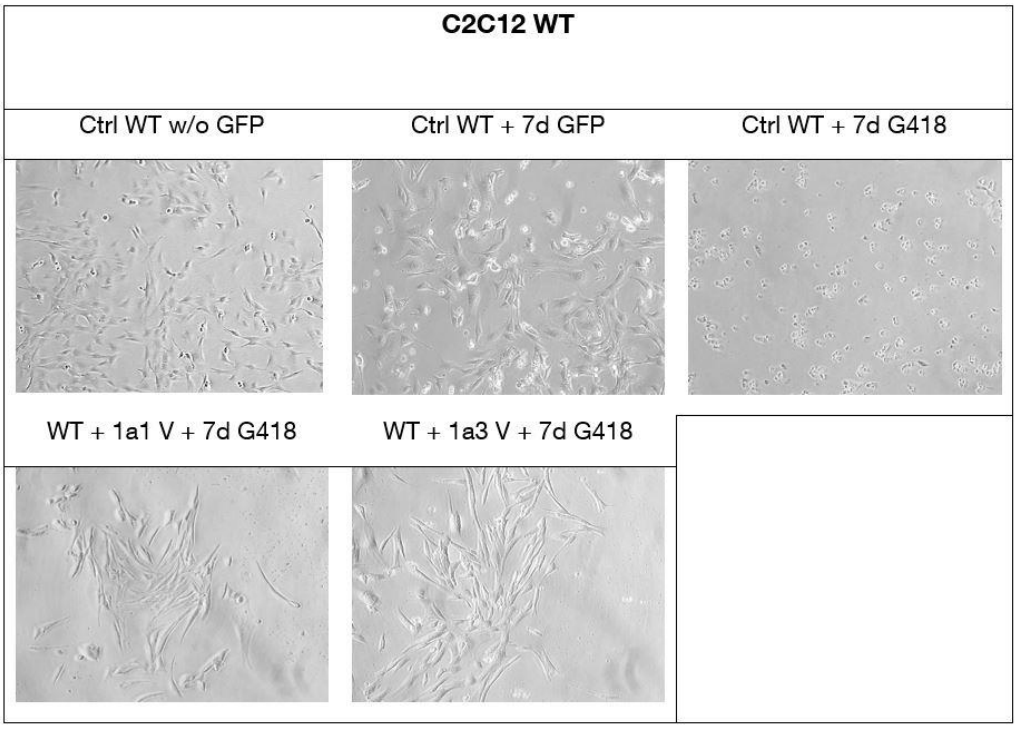

Figure 31: Microscopy of C2C12 Ctrl, C2C12 Ctrl transfected with GFP, C2C12 Ctrl with G418-treatment and C2C12 with stable transfection of recombinant ALDH1A1 or ALDH1A3 overexpression vector and subsequent G418 selection (magnification: Ctrl, Ctrl G418 10x, Ctrl GFP, C2C12 Vector + G418 20x)

Transfected samples were consecutively analyzed on protein level in order to demonstrate recombinant ALDH1A1 and ALDH1A3 overexpression.

GFP protein could be detected in Ctrl GFP sample and depicted a 25 kDa protein band size (Figure 32). Non-transfected Ctrl as well as 1a1 V and 1a3 V, respectively, were lacking 25 kDa protein band indicating GFP.

Further analysis revealed that 1a1 V and 1a3 V samples expressed a fusion product of ALDH1 isoform protein and GFP-insert, that could be demonstrated using antibodies directed against transfected isoforms ALDH1A1 and ALDH1A3, respectively. Hence, 54 kDa of ALDH1A1 was added with 25 kDa of GFP resulting in a 79 kDa fusion product. Protein size 56 kDa of ALDH1A3 was added 25 kDa of GFP and yielded a 81 kDa fusion product (Figure 33).

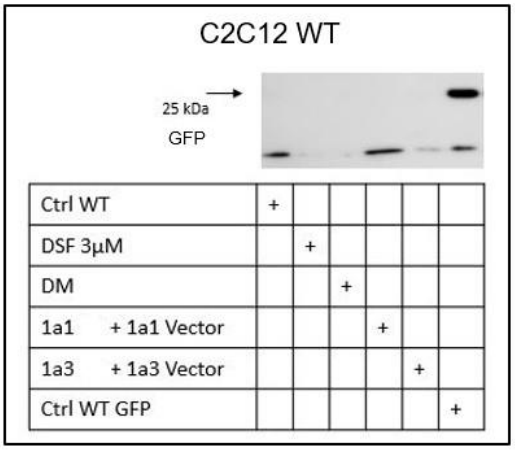

Figure 32: Anti-GFP Western Blot of C2C12 post stable transfection of recombinant ALDH1A1 or ALDH1A3 overexpression vector and consecutive G418 selection

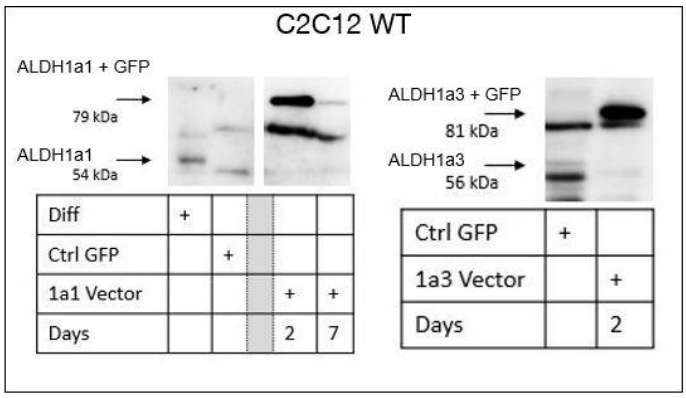

Figure 33: Anti-ALDH1a1 and –ALDH1a3 Western Blot of C2C12 post stable transfection of ALDH1a1 or ALDH1a3 overexpression vector and consecutive G418 selection

Since transfected samples 1a1 V and 1a3 V demonstrated a morphological change as already shown in Figure 31, samples were analyzed using antibodies against myogenic differentiation marker myogenin. 1a1 V as well as 1a3 V exposed an accumulated protein level of myogenin 2 days post transfection (Figure 34).

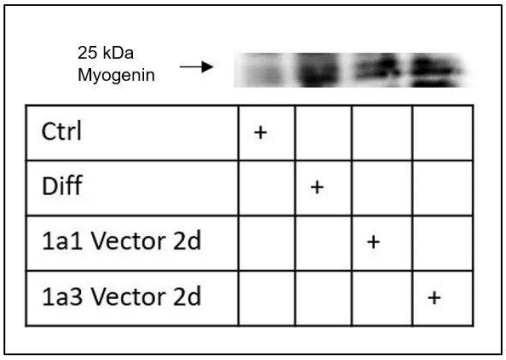

Figure 34: Anti-Myogenin Western Blot of C2C12 wildtype cells after stable transfection with recombinant ALDH1A1 or ALDH1A3 overexpression vector and G418 selection

6. Morphology of ALDH 1a1 Ko and ALDH 1a3 Ko Cells

In order to analyze the functional role of ALDH1 isoforms ALDH1A1 and ALDH1A3 in myogenic growth, genomic knockouts of ALDH1A1 and ALDH1A3, respectively, were performed in C2C12 and RH30 cell lines. Procedure was described in chapter 6 of Material and Method.

C2C12 ALDH1A1/ ALDH1A3 knockout (1a1 ko, 1a3 ko) and RH30 1A1/ 1A3 ko seemed to develop more protrusions than observed before in wildtype controls.

In Figure 35 C2C12 1a1 ko and 1a3 ko are depicted. Both C2C12 isoform ko groups were treated for several days with either DSF or serum-withdrawal in order to induce differentiation process. Though, no morphological changes could be observed in either group.

RH30 1a1 ko and 1a3 ko (Figure 36) demonstrated a comparable behavior. RH30 ko groups were treated with DSF or serum-withdrawal for several days as well, but no morphological changes could be noticed.

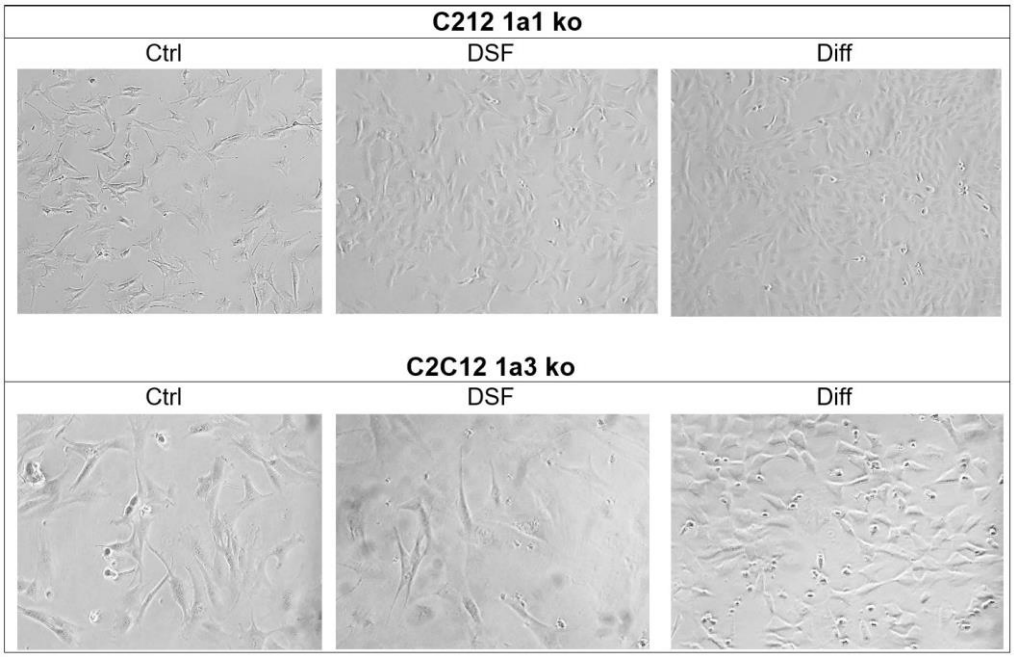

Figure 35: Captures of C2C12 ALDH 1a1 ko and 1a3 ko cells in diverse states

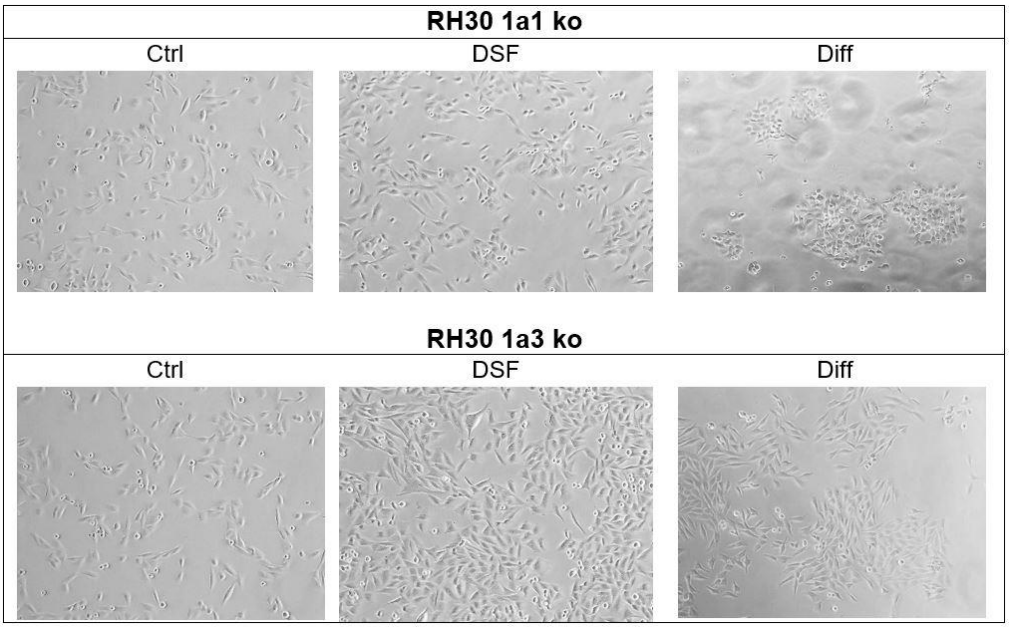

Figure 36: Captures of RH30 ALDH 1a1 ko and 1a3 ko cells in diverse states

Since no morphological change could be induced by serum-withdrawal, exemplary RH30 1a1 ko underwent serum-withdrawal for 3 days with a subsequent serum-restock for 3 days (Figure 37). The condition of high serum cultivation increased confluence of RH30 1a1 ko consecutively, which indicates proliferation process.

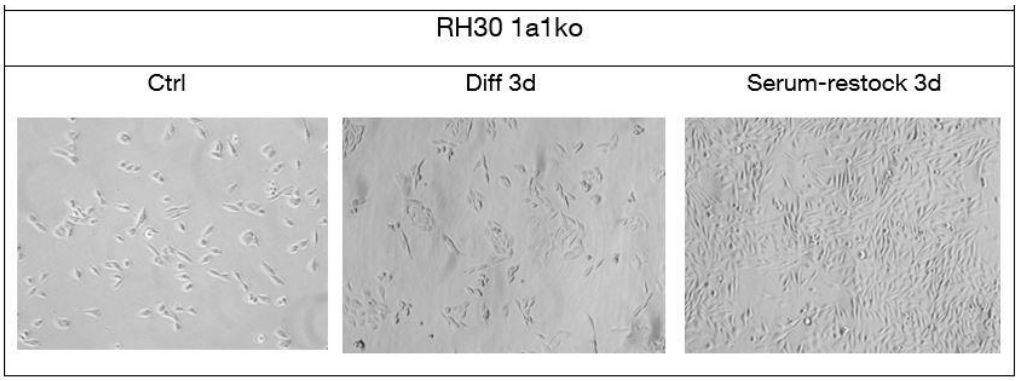

Figure 37: Capture of RH30 ALDH 1a1 ko cells with serum-restock after withdrawal

7. Protein Analysis of Ko Cells

C2C12 and RH30 1a1 ko/ 1a3, respectively, were analyzed after single cell colony purification. Using antibodies directed against ALDH1A1, ALDH1A3 and myogenic differentiation protein levels of ko samples were examined. Wildtype samples of C2C12 and RH30 were included as Ctrls.

C2C12 1a1 ko showed a strong knockdown effect of ALDH1A1 protein. In RH30 1a1 ko no ALDH1A1 protein was shown and therefore, demonstrated ALDH1A1 protein knockout (Figure 38).

As shown in Figure 39, samples of C2C12 and RH30 1a3 ko, respectively, demonstrated no protein of ALDH1a3 as well.

Differentiation behavior of serum-withdrawn samples was examined in all ko groups using antibodies against myogenic differentiation (Figure 40). Regardless the type of isoform ko

(1a1, 1a3) and cell line (RH30, C2C12) serum-withdrawn condition did not evoke protein accumulation of myogenin and hence, indicated no differentiation process.

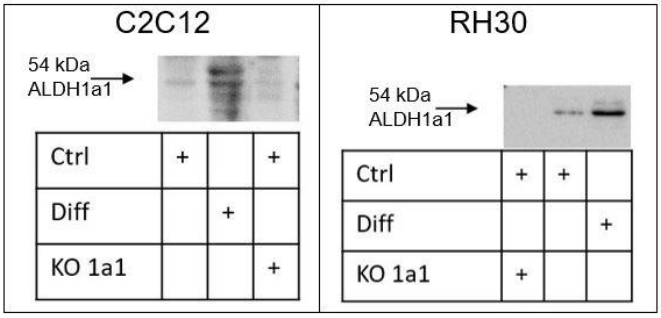

Figure 38: Anti-ALDH1A1 Western Blot of C2C12 1a1 ko and RH30 1a1 ko including controls

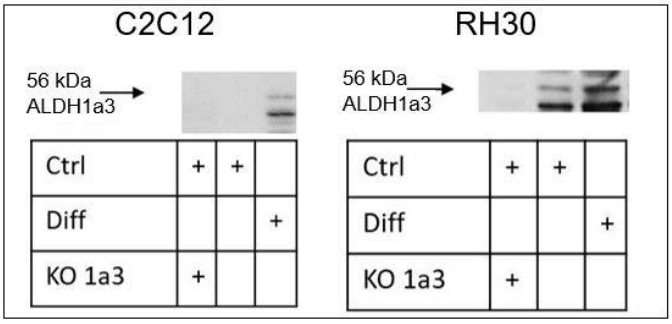

Figure 39: Anti-ALDH1A3 Western Blot of C2C12 1a3 ko and RH30 1a3 ko including controls

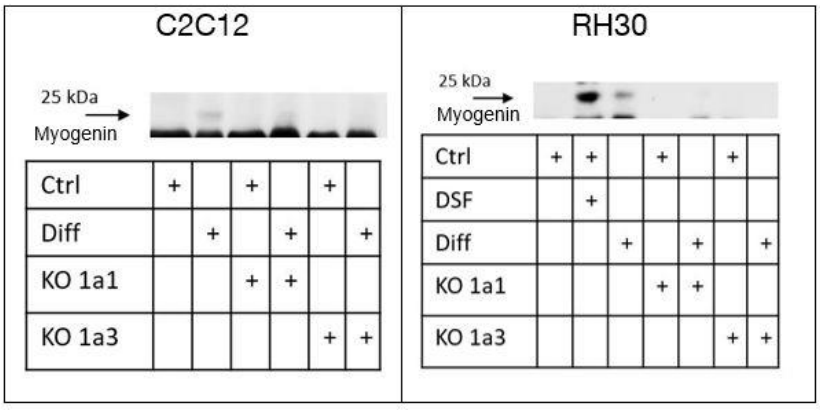

Figure 40: Anti-Myogenin Western Blot of C2C12 ko and RH30 ko including controls

8. ALDH1 Activity Analysis

In order to prove genomic ALDH1 activity knockout, Aldelfuor Assay was performed in C2C12 and RH30 1a1 and 1a3 ko, respectively (Figure 41). Since Aldefluor Assay does not distinguish between different ALDH1 isoforms, generic ALDH1 activity in ko groups was evaluated.

C2C12 1a1 ko and 1a3 ko depicted an enzymatic ALDH1 activity level of about 1 %. Compared to that wildtype cells yielded 55 % of ALDH1 activity (Figure 27).

RH30 1a1 ko and 1a3 ko showed an enzymatic ALDH1 activity of about 0.1 %; in comparison wildtype cells depicted 28% activity.

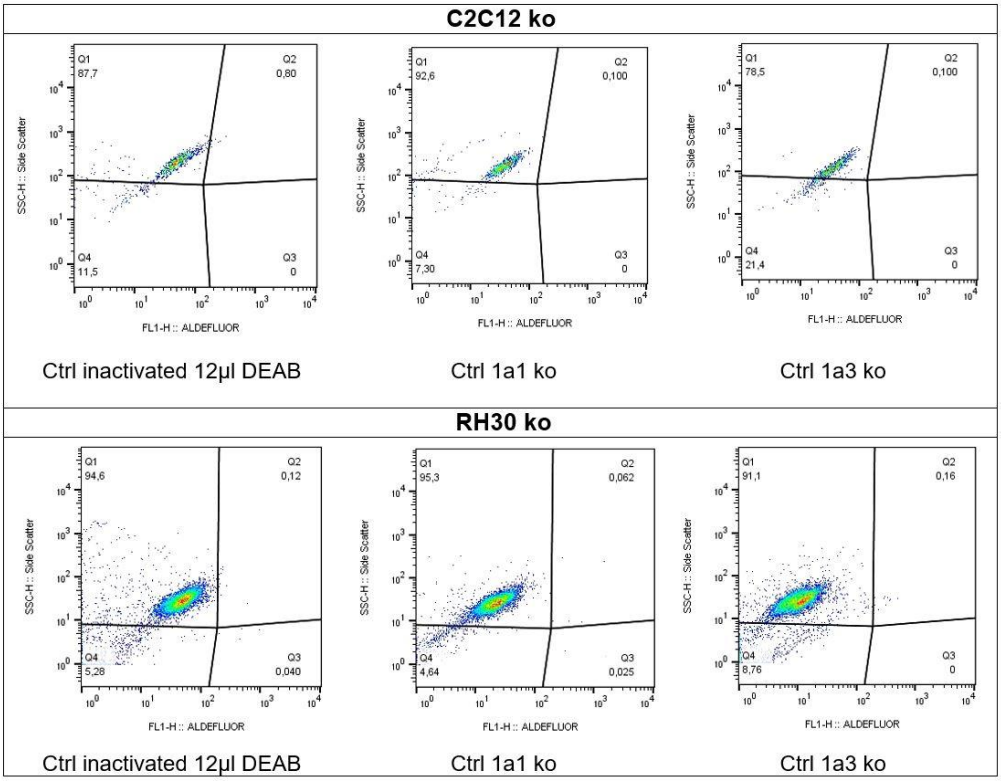

Figure 41: Aldelfuor Assay with C2C12 and RH30 isoform knockout

9. Immunofluorescent Staining Pattern of Ko Cells

In order to examine the expression pattern of ALDH1A1, ALDH1A3 and myogenic differentiation markers in ko groups of C2C12 and RH30, immunofluorescent staining was performed. Samples were cultivated on chamber slides and treated with serum-withdrawal or DSF for several days.

C2C12 and RH30 1a1 ko and 1a3 ko, respectively, illustrated no immunoreaction to anti-ALDH1A1 and anti-ALDH1A3 antibody (Figure 42, Figure 43). To be compared, wildtype cell lines demonstrated distinct variations of ALDH1 isoform expression depending on the treatment (Figure 28).

In detail, C2C12 1a1 ko did not show ALDH1A1 expression as well as C2C12 1a3 ko demonstrated no ALDH1A3. Both C2C12 ko groups did not increase ALDH1 isoform expression by treatments of DSF and serum-withdrawal. (Figure 42)

RH30 1a1 ko showed weak positivity for ALDH1A1 but depicted in comparison to wildtype RH30 cells a strong knockdown effect. RH30 1a1 ko did not increase expression signal of ALDA1A1 post treatments of DSF and serum-withdrawal. RH30 1a3 ko depicted no immunofluorescent expression of ALDH1A3, regardless the treatment. (Figure 43)

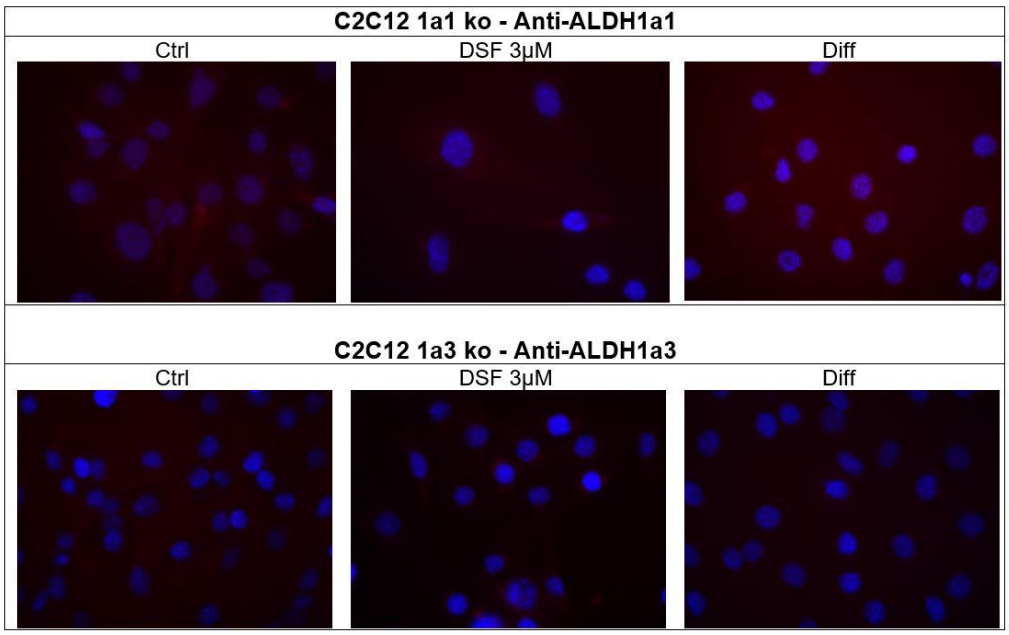

Figure 42: Immunofluorescent staining against ALDH1A1/ ALDH1A3 in C2C12 1a1 ko and 1a3 ko

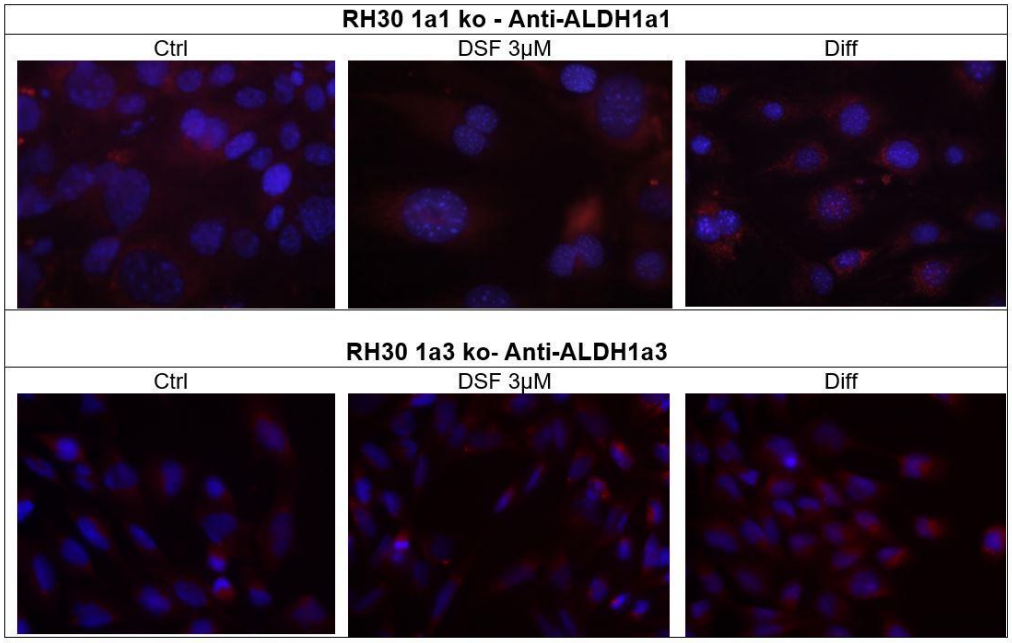

Figure 43: Immunofluorescent staining against ALDH1A1/ ALDH1A3 in RH30 1a1 ko and 1a3 ko

For validation of differentiative behavior anti-α-Aktin antibody reaction was investigated in samples of DSF-treatment and serum-withdrawal (Figure 44, Figure 45).

C2C12 and RH30 1a1 ko and 1a3 ko, respectively, were lacking immunoreaction to anti-α-Aktin antibody regardless the treatment.

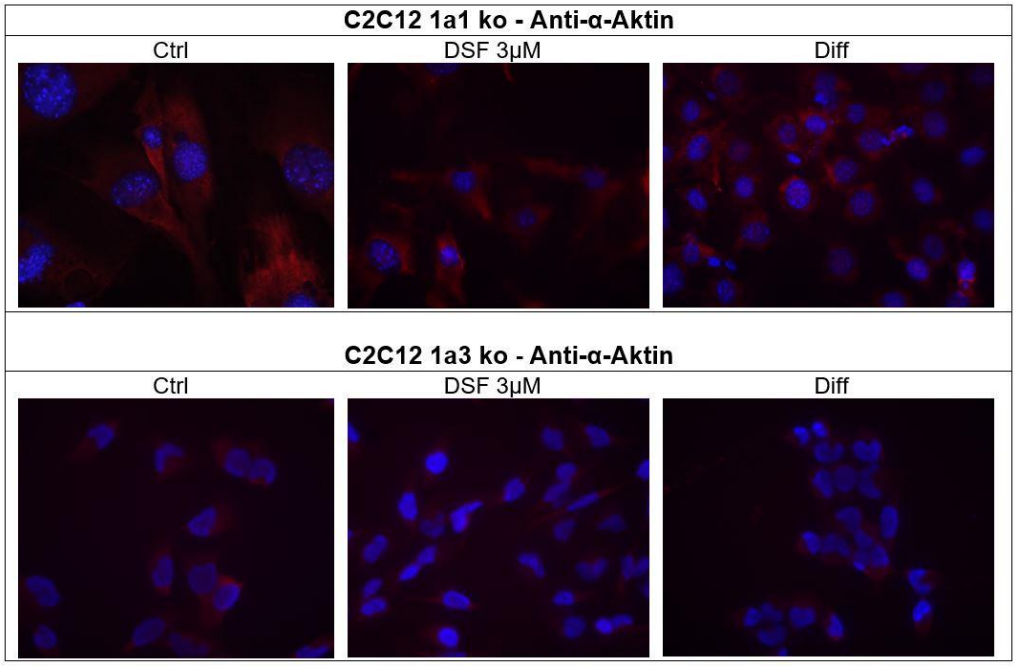

Figure 44: Immunofluorescent staining against α-Aktin in C2C12 1a1 ko and 1a3 ko (Magnification: 40x)

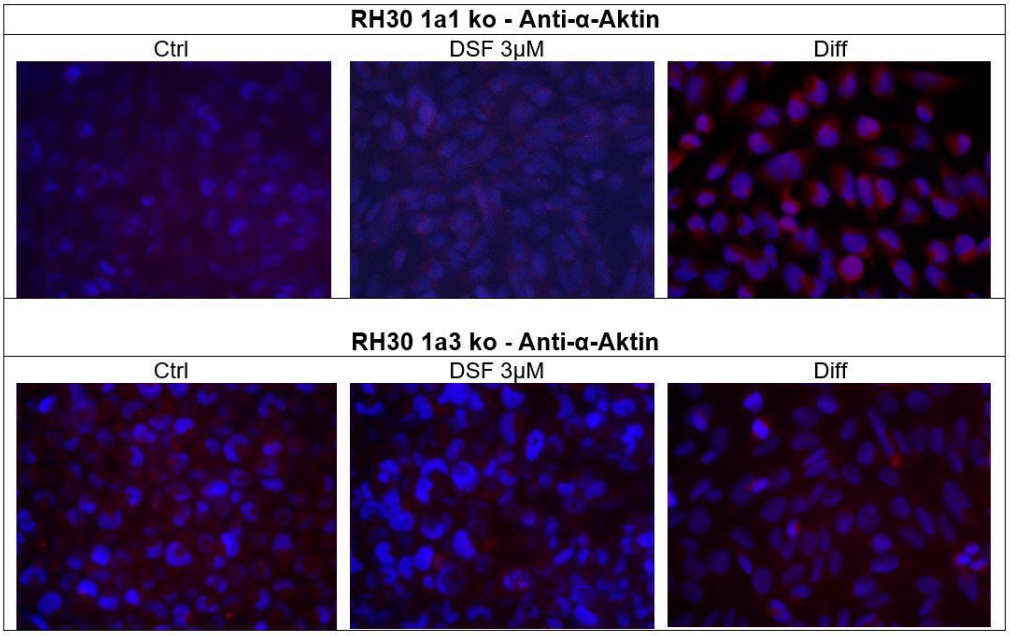

Figure 45: Immunofluorescent staining against α-Aktin in RH30 1a1 ko and 1a3 ko (magnification: 20x)

10. Re-transfection of Recombinant ALDH1 Isoform in Corresponding C2C12 Ko Cells

Previous experiments proved in C2C12 and RH30 1a1 ko and 1a3 ko, respectively, genomic knockout of ALDH1 isoform activity and impaired differentiative behavior. In the following experiments exemplary C2C12 ko groups were transfected with recombinant ALDH1A1 and ALDH1A3, respectively, for the recovery of ALDH1 isoforms activity.

10.1. Morphological Alteration

After stable transfection and G418-purification, the morphology of transfected C2C12 1a1 ko and 1a3 ko demonstrated after 7 days an elongated shape comparable to differentiated wildtype cells (Figure 46).

Exemplary transfection of GFP in ko control and treatment of G418 in a second ko control, demonstrated no morphological changes and hence were not inducer of adapted cell behavior.

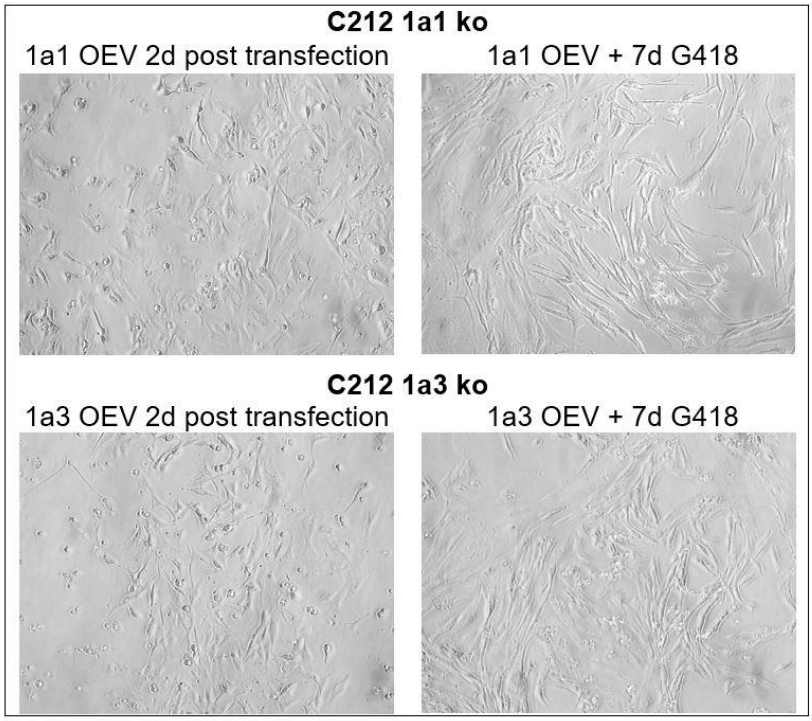

Figure 46: Capture of C2C12 knockout cells with ALDH re-transfection (magnification: 20x)

10.2. Protein Analysis of Re-Transfected Ko Cells

In order to prove a restoral of ALDH1A1 and ALDH1A3, respectively, expression, re-transfected samples of C2C12 1a1 ko and C2C12 1a3 ko were examined on protein level and are described as rescue samples.

Exemplary GFP ko controls depicted a 25 kDa protein band in anti-GFP antibody blotting (Figure 47). Rescue samples did not illustrate a GFP-specific protein band with a size of 25 kDa.

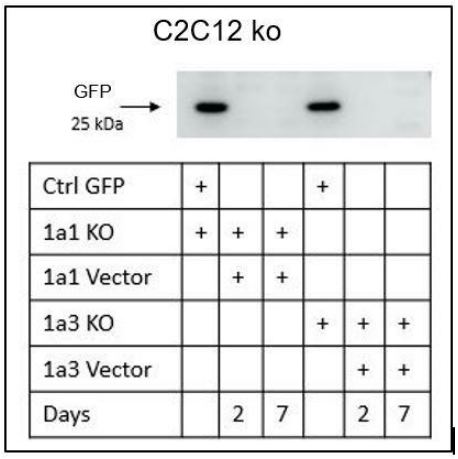

Figure 47: Anti-GFP Western Blot of C2C12 ko control, GFP-transfection and ALDH rescue

GFP control illustrated no ALDH1A1 or ALDH1A3 protein band on standard level (ALDH1A1: 54 kDa, ALDH1A3: 56 kDa) due to persistent ko of ALDH1A1 and ALDH1A3, respectively. ALDH1A3 positive control LN229 was indicating a 56 kDa band (Figure 48). Rescue samples did not demonstrate a GFP-protein band with a 25 kDa size. Consecutively, samples were examined with antibodies against ALDH1A1 and ALDH1A3 (Figure 48) and depicted a fusion product of GFP protein (25kDa) and ALDH1A1 (54 kDa) or ALDH1A3 (56 kDa), respectively. Here, band size was resulting again in a total protein band of 79 kDa or 81 kDa.

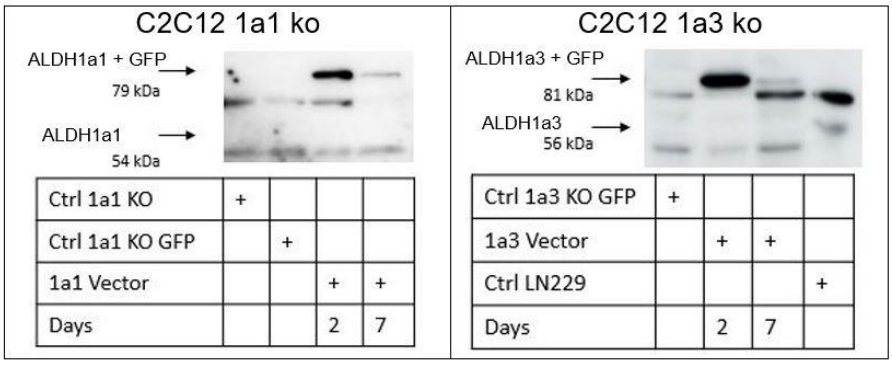

Figure 48: Anti-ALDH1A1 and -ALDH1A3 Western Blot of ko control, GFP control and ALDH rescue in ko

Since adaptive morphology change could be observed, anti-Myogenin antibody analysis was performed for examination of differentiation in rescue samples (Figure 49).

Rescue samples depicted 2 days post transfection not accumulation of myogenin protein, whereas 7 days post transfection protein of myogenin band size was shown and indicating differentiation process.

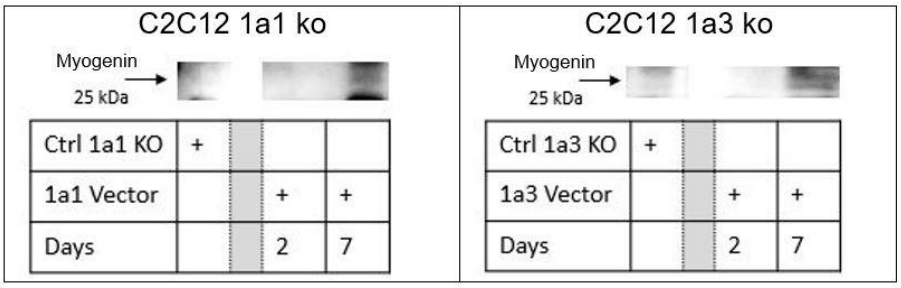

Figure 49: Anti-Myogenin Western Blot of C2C12 1a1 ko and 1a3 ko control and ALDH rescue

10.3. ALDH1 Activity Restoral

Recombinant ALDH1 isoform restoral could be proven on protein level in ko groups of C2C12. In order to examine additional recovery of enzymatic ALDH1 activity, Aldefluor Assay was performed.

In exemplary C2C12 1a1 ko rescue ALDH1 enzyme activity has slightly accelerated upon day 2 post re-transfection of recombinant ALDH1A1 plasmid (Figure 50). Since recombinant

overexpression already lead to differentiation (Figure 49), additional treatment of serum-withdrawal was excluded from this experiment.

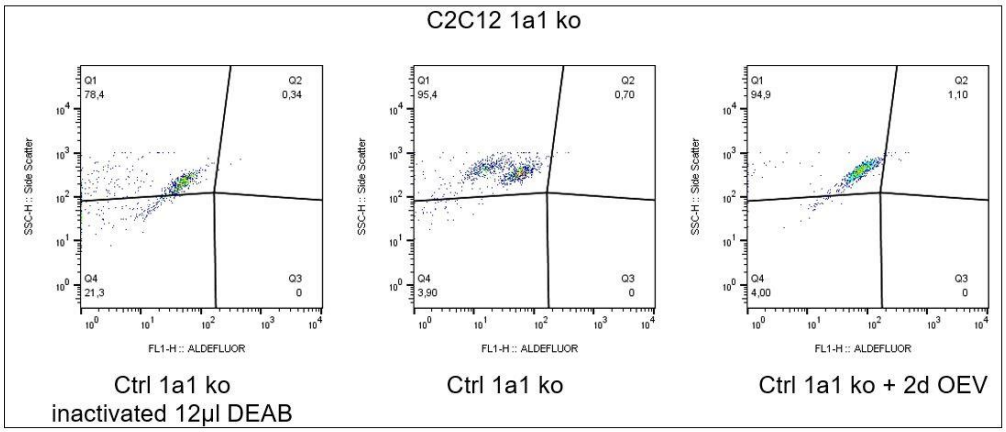

Figure 50: Aldefluor Assay analysis of C2C12 1a1 ko with recombinant ALDH1A1 rescue (Ctrl 1a1 ko + 2d OEV)

F. Discussion

The process of myogenic growth relies on the activation and action of satellite cells (SCs), which constitute the stem cell population in skeletal muscle. Unique characteristics of stem cells are the ability to return to quiescent status and the potential of self-renewal. Considering that musculature depicts a terminally differentiated organ, SCs are the important resource of skeletal muscle homeostasis.

SC action is induced by environmental stimuli and is then aiming for growth, differentiation and repair of skeletal muscle. For instance, low doses of oxidative stress, exemplarily induced by physical activity leads to adaptive growth performed by SCs (Abruzzo et al., 2013; Musarò et al., 2010). In contrast, high oxidative stress levels are generated by forms of insult or inflammation and promote SC activation for cellular repair (Vella et al., 2011). Both adaptive growth behavior and regenerative processes demand the development of muscle structure and hence, requires the activation of SCs.

Previously, the enzyme Aldehyde Dehydrogenase 1 (ALDH1) was identified as regulator of differentiation and as protector of cellular capability, since isoforms ALDH1A1 and ALDH1A3 are determinants in RA signaling, which then is regulating differentiation (Gudas, 2012) and detoxifying agents of oxidative stress and lipid peroxidation products (Fritz & Petersen, 2013; Le Moal et al., 2017). Most recently, I could demonstrate the co-localization of isoforms ALDH1A1 and ALDH1A3 in SCs of human skeletal muscle tissue (Rihani et al., submitted data). Although, findings corroborate ALDH1 isoforms as important factors in myogenesis and muscle homeostasis, the functional role of ALDH1A1 and ALDH1A3 in skeletal muscle development and SC activation is yet not characterized.

The present data shows, that ALDH1 isoforms ALDH1A1 and ALDH1A3 are pivotal factors in myogenic differentiation, since increased levels of ALDH1 enzyme activity and high ALDH1A1 and ALDH1A3 protein levels could be demonstrated upon myotube formation. Differentiation

process could be induced by recombinant overexpression of ALDH1A1 and ALDH1A3, respectively. In contrast, differentiation ability perishes in ALDH1A1 and ALDH1A3 deficient skeletal muscle cells and could be recovered by subsequent re-transfection of recombinant ALDH1A1 and ALDH1A3, respectively. Most interestingly, enzymatic ALDH inhibition evoked differentiation as well and demonstrated increased ALDH1A1 and ALDH1A3 protein levels.

In order to explain the functional role of ALDH1A1 and ALDH1a3 in myogenesis in more detail, I will discuss the present data in the context of recent studies.

1. Increased ALDH1A1 and ALDH1A3 Activity indicates Myogenic Differentiation

Previous studies identified enzyme ALDH1 as hallmark of myogenic capacity in subpopulations of muscle progenitors (Vauchez et al., 2009). Therefore, ALDH1 isoforms ALDH1A1 and ALDH1A3 were investigated in murine C2C12 and human RH30 myoblast cell lines on the basis of established myogenic differentiation markers (Mukund & Subramaniam, 2020). C2C12 and RH30 are widely accepted myoblast cell lines and accepted as satellite cell-like models, since the development of myoblast into terminally differentiated myotubes can be induced by serum-withdrawal.

Here, subsequent differentiation could be confirmed by myogenic differentiation markers (Figure 26, Figure 29). Consecutive analysis of ALDH1 isoforms revealed increased protein levels of ALDH1A1 and ALD1A3, respectively, upon myotube formation (Figure 25). In Aldefluor Assay ALDH activity level was remarkably higher in differentiated cells; in detail, C2C12 depicted an increase of more than 30 % positivity and RH30 more than 40 % (Figure 27). Immunofluorescent staining demonstrated comparable results, illustrating in differentiation an increased immunoreaction to antibodies against ALDH1A1 and ALDH1A3, respectively (Figure 28).

A congruent presence of myogenic differentiation marker and ALDH1A1 and ALDH1A3, respectively, could be demonstrated in C2C12 and RH30 cells. Hence, ALDH1A1 and ALDH1A3 upregulation could be included for the demonstration of myogenic differentiation process.

As Vauchez, Marolleau et al., stated, skeletal muscle subpopulations with high levels of ALDH1 depict high myogenic capacities, especially in regard of differentiation processes. Here, I could demonstrate that ALDH1 isoforms ALDH1A1 and ALDH1A3 are predominantly active in differentiation. Further experiments in this project will address the detailed functional role of ALDH1A1 and ALDH1A3 in myogenic differentiation.

2. Enzymatic ALDH Inhibition leads to ALDH1A1 and ALDH1A3 Protein Accumulation and Consecutive Differentiation

Since prior results demonstrated a predominant presence of ALDH1A1 and ALDH1A3 in differentiation, conditions of temporary enzymatic ALDH inhibition using chemical Disulfiram (DSF) was investigated in C212 and RH30 cell lines.

Interestingly, enzymatic ALDH inhibition did not prohibit differentiation. Instead, the formation of elongated myotubes was observed in consecutive DSF-treated cells (Figure 24) and myogenic differentiation markers proved differentiation in Western Analysis (Figure 26) as well as in Immunofluorescence (Figure 29). Furthermore, a multiple day inhibition of ALDH enzyme leads to accumulated protein levels of ALDH1A1 and ALDH1A3 (Figure 25) and additional increased ALDH1A1 and ALDH1A3 immunoreaction in immunofluorescence (Figure 28).

Findings demonstrate an increased aggregation of ALDH1 protein due to functional inability by enzymatic DSF treatment. High levels of ALDH1A1 and ALDH1A3 protein induces myogenic differentiation behavior, although ALDH1 isoforms were chemically blocked and no serum-withdrawal was applied.

A similar phenomenon was demonstrated in experimental studies of Wu et al., 2020, who showed increased levels of ALDH1A3 in Temozolomide (TMZ) treated recurrent glioblastoma tumors. They showed that chemotherapeutic drug TMZ initially reduced levels of ALDH1A3, but after finishing treatment period ALDH1A3 was dramatically increasing to levels even higher than pre-treatment. Enzyme ALDH1A3 is associated with poor response to TMZ treatment in glioblastoma brain tumor patients. TMZ is primarily targeting cancer cells by increased oxidative stress production, but ALDH1A3 is strongly increases in a delayed manner due to its detoxifying function.

My results seem to be in line with these findings, since the chemically induced reduction of ALDH1 isoform function evokes a delayed significant upregulation of ALDH1 isoforms. Further experiments should further investigate the regulatory mechanism of conditional ALDH1 inhibition in myogenic differentiation.

3. Recombinant Overexpression of ALDH1A1 and ALDH1A3 Isoforms induces Myotube Formation

Since ALDH1 activity is linked to myogenic differentiation, C2C12 cells were cultivated in standard conditions and subsequently transfected with recombinant ALDH1A1 and ALDH1A3, respectively, for overexpression.

Stable transfected cells demonstrated a higher protein amount of ALDH1 isoforms than non-transfected control samples (Figure 33). Recombinant overexpression of ALDH1A1 and ALDH1A3, respectively, induced differentiative behavior in muscle cells (Figure 31) and was proven on protein level using myogenic differentiation marker (Figure 34).

Interestingly, differentiation was induced despite serum-withdrawal was not applied. High levels of ALDH1A1 and ALDH1a3 protein are again associated with myogenic differentiation behavior.

Few studies were addressing the function of ALDH activity in myogenic development. For instance, Etienne et al., 2020, recently identified ALDH bright muscle progenitor cells to be remarkably high myogenic in regard of muscle stability and regeneration. They analyzed human muscle cells in Aldefluor Assay and categorized them in low and high ALDH positivity. ALDH1A1 and ALDH1A3 activity was emphasized as important factors in muscle homeostasis. My results define the molecular mechanism of ALDH1A1 and ALDH1A3 in myogenesis in more detail, since not only the enzymatic activity of ALDH1, but also the functional role of ALDH1 was examined. The application of recombinant ALDH1A1 and ALDH1A3 overexpression is a novel approach for the investigation of ALDH1 isoform mechanism in myogenic differentiation.

4. Genomic Knockout of ALDH1A1 and ALDH1A3 impairs Differentiation

Previous results (chapters 1, 2, 3 of Discussion) corroborate the role of ALDH1 being a predominant factor in myogenic differentiation, since the accumulation of ALDH1A1 and ALDH1A3 protein seems to be the basis of differentiation processes. In summary, myotube formation could be evoked by serum-withdrawal, chemical ALDH inhibition and recombinant ALDH1A1 and ALDH1A3 overexpression. Though, it is still not clear how ALDH1 isoforms are functionally modulating myogenic differentiation.

Genomic ALDH1A1 and ALDH1A3, respectively, knockout in C2C12 and RH30 cell lines allows the direct examination of ALDH1 isoforms function myogenic growth.

Knockout cell lines with deficient ALDH1A1 (1a1 ko) and ALDH1A3 (1a3 ko), respectively, were analyzed in Western Blot and Immunofluorescence using antibodies against ALDH1A1 in 1a1 ko and ALDH1A3 in 1a3 ko. Knockout effects could be proven on protein level (Figure 38, Figure 39) and lacking immunofluorescent staining pattern (Figure 42, Figure 43). Additional Aldefluor Assay demonstrated low enzymatic ALDH1 activity in ko cell lines with solely 1 % ALDH active cells (Figure 41).

Consecutive experiments were analogously performed as in wildtype cell lines. As expected, serum-withdrawal depicted no effects on morphology in 1a1 ko and 1a3 ko C2C12 and RH30, respectively (Figure 35, Figure 36). Furthermore, in Western Analysis deficient myogenic differentiation marker could be observed (Figure 40). Additional, immunofluorescent staining using antibodies against myogenic differentiation marker revealed no expression patterns indicating differentiation (Figure 44, Figure 45). DSF-treated C2C12 and RH30 1a1a ko and 1a3 ko, respectively, did not show differentiation behavior as well (Figure 35, Figure 36).

Moreover, a restoral of high-serum conditions evoked in previously serum-withdrawn RH30 1a1 ko cells an increasing confluence, which is indicating no terminal differentiation by serum-withdrawal (Figure 37).

Altogether, C2C12 and RH30 cells with genomic 1a1 ko and 1a3 ko demonstrate the inability to differentiate. Since, chemical inhibition of ALDH in wildtype cells did not eliminate protein levels of ALDH1A1 and ALDH1A3, differentiation process could not be impaired. In contrast, ko cells were lacking protein of ALDH1A1 and ALDH1A3, respectively. Depletion of ALDH1A1 and ALDH1A3 protein seems to be the reason for the loss of differentiation ability.

Conclusively, protein of isoforms of ALDH1A1 and ALDH1A3, respectively, are essential determinants in the process of myogenic differentiation.

5. Re-transfection of ALDH1A1 and ALDH1A3 in C2C12 1a1 ko and 1a3 ko Recovers Ability to Differentiate

Since genomic knockout of ALDH1A1 and ALDH1A3, respectively, leads to impaired protein in muscle cells and subsequent loss of differentiation, recombinant re-expression of ALDH1A1 and ALDH1A3, respectively, in C2C12 ko was performed.

Re-transfected C2C12 1a1 ko and 1a3 ko cells depicted recovered ALDH1 isoforms with even higher protein levels than in observed wildtype controls (Figure 48).Two days post re-transfection in ko cells, ALDH activity level was measured and already described a slight ALDH activity increase (Figure 50). Stable re-expression of ALDH1A1 and ALDH1A3, respectively, induced differentiation process in former C2C12 1a1 ko and 1a3 ko cells (Figure 46). Subsequently, differentiation could be confirmed on protein level using an antibody directed against myogenic differentiation marker (Figure 49).

Conclusively, genomic knockout of ALDH1 isoforms impairs the ability to form myotubes in muscle cells, whereas a rescue of ALDH1A1 and ALDH1A3 protein expression recovers the potential of differentiation.

Experimental setup of ALDH1 isoform knockout cells and consecutive recombinant re-expression of ALDH1A1 and ALDH1A3, evidence the pivotal role of ALDH1 isoform proteins in myogenic differentiation. Since genomic knockout and re-transfection of ALDH1A1 and ALDH1A3 isoforms was performed in separated cell groups, it can be stated that both isoforms, ALDH1A1 and ALDH1A3, are equally important for the ability to differentiate.

6. Conclusion

ALDH1 isoforms ALDH1A1 and ALDH1A3 are not only pacemakers in oxidative stress situations and regulators of RA signaling, but also directly dedicate the ability of myogenic differentiation. ALDH1A1 and ALDH1A3 depletion renders muscle cells unable to differentiate. The process of myogenesis relies on environmental stimuli affecting SCs for activation and consecutive growth behavior. Here, it is shown that ALDH1A1 and ALDH1A3 protein accumulation can induce differentiation in muscle cells as well. Interestingly, chemical inhibition of ALDH1 is also affecting myogenic differentiation by protein aggregation of isoforms ALDH1A1 and ALDH1A3. In contrast, genomic knock out of isoforms ALDH1A1 and ALDH1A3, respectively, and consecutive depletion of ALDH1 isoform proteins is the limiting factor in differentiation. Moreover, re-transfection of recombinant ALDH1A1 and ALDH1a3 in ko cells recovers defective differentiation phenotype. Thus, protein expression of ALDH1A1 and ALDH1A3 are crucial for the process of myotube formation. These findings demonstrate the essential role of ALDH1A1 and ALDH1A3 in myogenesis, in particular myogenic differentiation. This conclusion fosters ALDH1 isoforms as potential SC activators, since I could recently demonstrate their co-localization in human SCs. Furthermore, this finding supports the establishment of new approach in skeletal muscle repair and skeletal muscle tumor therapy.

G. Acknowledgement

Ich danke allen lieben Menschen, die mich bis hierher begleitet haben und mir mit Rat und Zuspruch zur Seite standen. Diese Jahre waren so ereignisreich wie wundervoll.

Allen voran möchte ich mich bei meinem Doktorvater Jürgen Schlegel für all die schönen Jahre in deiner Arbeitsgruppe Neuro bedanken. Ich nehme so Vieles mit und danke dir für dein offenes Ohr, deine Ratschläge und deine stets ehrliche Kritik. Ich sage stets, dass ich in diesen Jahren erwachsen geworden bin. In dieser Zeit wurde aus einer Bachelor Thesis eine Master Thesis und letztendlich auch ein Doktorprojekt. Kaum woanders als in deinem Team und Labor habe ich mehr Zeit verbracht und dazu auch noch gerne.

Außerdem möchte ich mich bei meinem Mann Maroan für all die Stunden bedanken in denen du Höhen und Tiefen mitgemacht und mir den Rücken gestärkt hast. Deine Bewunderung für meine Forschung und dein Zuspruch haben es mir ermöglicht bis hierher zu kommen.

Ohne meine lieben Kolleginnen Fritzi und Sandra, als auch all den anderen, die diese Arbeitsgruppe erst zum Leben erwecken, wären diese Jahre bei weitem nicht so wundervoll geworden. Es waren in diesen Jahren so viele liebe Menschen Teil dieser Gruppe, sodass ich leider nicht alle einzeln nennen kann.

Ich bedanke mich auch bei all meinen Freunden für tolle Gespräche, Diskussionen und schöne Erlebnisse. Durch euch konnte ich immer wieder neue Kraft finden und mein Bestreben weiter ausbauen. Auch hier kann ich nicht alle nennen, da ich dankenswerterweise sehr viele liebe Menschen an meiner Seite weiß und hoffe, dass sich alle angesprochen fühlen.

Ebenso danke ich meinen lieben Schwiegereltern, besonders bei meiner lieben Nadja, die stets mitgefiebert und mich zu neuen und höheren Zielen motiviert hat.

Zu guter Letzt möchte ich mich natürlich bei meiner Familie bedanken; meinem geliebten Bruder Philipp und meinen lieben Eltern Sigrid und Benedikt. Danke für eure aufopfernde Fürsorge über all die Jahre und die mich teilweise bis hierhergebracht hat. Auch wenn es nicht immer leicht war, seid ihr Teil meines Herzens und ich bin froh mit euch nun diesen Weg wieder gemeinsam gehen zu können.

Meine hier zu Papier gebrachte Dissertation möchte ich allerdings einem ganz besonderen Menschen widmen. Jemandem, der mich lange im Leben begleitet hat und auch bis heute fester Bestandteil in meinem Herzen ist. Diese Zeilen sind für dich, geliebte Tante Christl. Du fehlst jeden Tag.

H. References

Abruzzo, P. M., Esposito, F., Marchionni, C., Di Tullio, S., Belia, S., Fulle, S., Veicsteinas, A. & Marini, M. (2013). Moderate exercise training induces ROS-related adaptations to skeletal muscles. *International journal of sports medicine*, *34*(8), 676–687, doi: 10.1055/s-0032-1323782.

Albagli-Curiel, Olivier, Carnac, Gilles, Vandromme, Marie, Vincent, Sylvie, Crépieux, Pascale & Bonnieu, Anne (1993). Serum-induced inhibition of myogenesis is differentially relieved by retinoic acid and triiodothyronine in C2 murine muscle cells. *Differentiation*, *52*(3), 201–210, doi: 10.1111/j.1432-0436.1993.tb00632.x.

Alric, S., Froeschlé, A., Piquemal, D., Carnac, G. & Bonnieu, A. (1998). Functional specificity of the two retinoic acid receptor RAR and RXR families in myogenesis. *Oncogene*, *16*(2), 273–282, doi: 10.1038/sj.onc.1201484.

Amuchastegui, Tomas, Amuchastegui, Marcos & Donohue, Thomas (2014). Disulfiram--alcohol reaction mimicking an acute coronary syndrome. *Connecticut medicine*, *78*(2), 81–84. PMID: 24741856

Barlow, Jason W., Wiley, Joe C., Mous, Marieke, Narendran, Aru, Gee, Matthew F. W., Goldberg, Michael, Sexsmith, Elizabeth & Malkin, David (2006). Differentiation of rhabdomyosarcoma cell lines using retinoic acid. *Pediatric blood & cancer*, *47*(6), 773–784, doi: 10.1002/pbc.20650.

Benjamin D Cosgrove, Penney M Gilbert, Ermelinda Porpiglia, Foteini Mourkioti, Steven P Lee, Stephane Y Corbel, Michael E Llewellyn, Scott L Delp & Helen M Blau (2014). Rejuvenation of the muscle stem cell population restores strength to injured aged muscles. *Nature Medicine*, *20*(3), 255–264, doi: 10.1038/nm.3464.

Bert Blaauw & Carlo Reggiani (2014). The role of satellite cells in muscle hypertrophy. *Journal of Muscle Research and Cell Motility*, *35*(1), 3–10, doi: 10.1007/s10974-014-9376-y.

Black, William J., Stagos, Dimitrios, Marchitti, Satori A., Nebert, Daniel W., Tipton, Keith F., Bairoch, Amos & Vasiliou, Vasilis (2009). Human aldehyde dehydrogenase genes: alternatively spliced transcriptional variants and their suggested nomenclature. *Pharmacogenetics and genomics*, *19*(11), 893–902, doi: 10.1097/FPC.0b013e3283329023.

Cobb, Laura (2013). Cell Based Assays: the Cell Cycle, Cell Proliferation and Cell Death. *Materials and Methods*, *3, doi: 10.13070/mm.en.3.172*.

Crouch, G. D. & Helman, L. J. (1991). All-trans-retinoic acid inhibits the growth of human rhabdomyosarcoma cell lines. *Cancer research*, *51*(18), 4882–4887. PMID: 1893378

D'Ambrosio, Diana N., Clugston, Robin D. & Blaner, William S. (2011). Vitamin A Metabolism: An Update. *Nutrients*, *3*(1), 63–103, doi: 10.3390/nu3010063.

Ding, Shijie, Wang, Fei, Liu, Yan, Li, Sheng, Zhou, Guanghong & Hu, Ping (2017). Characterization and isolation of highly purified porcine satellite cells. *Cell death discovery*, *3*, 17003, doi: 10.1038/cddiscovery.2017.3.

Emanuele Marzetti, Riccardo Calvani, Matteo Tosato, Matteo Cesari, Mauro Di Bari, Antonio Cherubini, Agnese Collamati, Emanuela D'Angelo, Marco Pahor, Roberto Bernabei & Francesco Landi (2017). Sarcopenia: an overview. *Aging Clinical and Experimental Research*, *29*(1), 11–17, doi: 10.1007/s40520-016-0704-5.

Etienne, Jessy, Joanne, Pierre, Catelain, Cyril, Riveron, Stéphanie, Bayer, Alexandra Clarissa, Lafable, Jérémy, Punzon, Isabel, Blot, Stéphane, Agbulut, Onnik & Vilquin, Jean-Thomas (2020). Aldehyde dehydrogenases contribute to skeletal muscle homeostasis in healthy, aging, and Duchenne muscular dystrophy patients. *Journal of cachexia, sarcopenia and muscle.* Advance online publication, doi: 10.1002/jcsm.12557.

Feng, Xuesong, Naz, Faiza, Juan, Aster H., Dell'Orso, Stefania & Sartorelli, Vittorio (2018). Identification of Skeletal Muscle Satellite Cells by Immunofluorescence with Pax7 and Laminin Antibodies. *Journal of visualized experiments : JoVE.* Advance online publication, doi: 10.3791/57212.

Fiacco, E., Castagnetti, F., Bianconi, V., Madaro, L., Bardi, M. de, Nazio, F., D'Amico, A., Bertini, E., Cecconi, F., Puri, P. L. & Latella, L. (2016). Autophagy regulates satellite cell ability to regenerate normal and dystrophic muscles. *Cell death and differentiation*, *23*(11), 1839–1849, doi: 10.1038/cdd.2016.70.

Forcina, Laura, Miano, Carmen, Pelosi, Laura & Musarò, Antonio (2019). An Overview about the Biology of Skeletal Muscle Satellite Cells. *Current Genomics*, *20*(1), 24–37, doi: 10.2174/1389202920666190116094736.

Fritz, Kristofer S. & Petersen, Dennis R. (2013). An overview of the chemistry and biology of reactive aldehydes. *Free radical biology & medicine*, *59*, 85–91, doi: 10.1016/j.freeradbiomed.2012.06.025.

García-Prat, Laura, Martínez-Vicente, Marta, Perdiguero, Eusebio, Ortet, Laura, Rodríguez-Ubreva, Javier, Rebollo, Elena, Ruiz-Bonilla, Vanessa, Gutarra, Susana, Ballestar, Esteban, Serrano, Antonio L., Sandri, Marco & Muñoz-Cánoves, Pura (2016). Autophagy maintains stemness by preventing senescence. *Nature*, *529*(7584), 37–42, doi: 10.1038/nature16187.

García-Prat, Laura, Sousa-Victor, Pedro & Muñoz-Cánoves, Pura (2013). Functional dysregulation of stem cells during aging: a focus on skeletal muscle stem cells. *The FEBS journal*, *280*(17), 4051–4062, doi: 10.1111/febs.12221.

Gudas, Lorraine J. (2012). Emerging roles for retinoids in regeneration and differentiation in normal and disease states. *Biochimica et biophysica acta*, *1821*(1), 213–221, doi: 10.1016/j.bbalip.2011.08.002.

Guo K., Wang J, Andrés V. & et al. (1995). MyoD-Induced Expression of p21 Inhibits Cyclin-Dependent Kinase Activity upon Myocyte Terminal Differentiation. *Molecular Cell Biology*, *1995*(15), Artikel 7, 3823–3829, doi: 10.1128/mcb.15.7.3823.

Hang Yin, Feodor D. Price & Michael A. Rudnicki (2013). Satellite cells and the muscle stem cell niche. *Physiological reviews.* Advance online publication, doi: 10.1152/physrev.00043.2011.

Hernandez-Segura, Alejandra, Nehme, Jamil & Demaria, Marco (2018). Hallmarks of Cellular Senescence. *Trends in cell biology*, *28*(6), 436–453, doi: 10.1016/j.tcb.2018.02.001.

Hlaing, Myint, Shen, Xun, Dazin, Paul & Bernstein, Harold S. (2002). The hypertrophic response in C2C12 myoblasts recruits the G1 cell cycle machinery. *The Journal of Biological Chemistry*, *277*(26), 23794–23799, doi: 10.1074/jbc.M201980200.

Ito, Fumiaki, Sono, Yoko & Ito, Tomoyuki (2019). Measurement and Clinical Significance of Lipid Peroxidation as a Biomarker of Oxidative Stress: Oxidative Stress in Diabetes, Atherosclerosis, and Chronic Inflammation. *Antioxidants (Basel, Switzerland)*, *8*(3), doi: 10.3390/antiox8030072.

Jean, Elise, Laoudj-Chenivesse, Dalila, Notarnicola, Cécile, Rouger, Karl, Serratrice, Nicolas, Bonnieu, Anne, Gay, Stéphanie, Bacou, Francis, Duret, Cédric & Carnac, Gilles (2011). Aldehyde dehydrogenase activity promotes survival of human muscle precursor cells. *Journal of cellular and molecular medicine*, *15*(1), 119–133, doi: 10.1111/j.1582-4934.2009.00942.x.

Jiayi Huang, Rekha Chaudhary, Adam L. Cohen, Karen Fink, Samuel Goldlust, John Boockvar, Prakash Chinnaiyan, Leping Wan, Stephen Marcus & Jian L. Campian (2019). A multicenter phase II study of temozolomide plus disulfiram and copper for recurrent temozolomide-resistant glioblastoma. *Journal of Neuro-Oncology*, *142*(3), 537–544, doi: 10.1007/s11060-019-03125-y.

Jin, Na, Zhu, Xiaojian, Cheng, Fanjun & Zhang, Liling (2018). Disulfiram/copper targets stem cell-like ALDH+ population of multiple myeloma by inhibition of ALDH1A1 and Hedgehog pathway. *Journal of cellular biochemistry*, *119*(8), 6882–6893, doi: 10.1002/jcb.26885.

Kirkland, James L. & Tchkonia, Tamara (2017). Cellular Senescence: A Translational Perspective. *EBioMedicine*, *21*, 21–28, doi: 10.1016/j.ebiom.2017.04.013.

Kozakowska, Magdalena, Pietraszek-Gremplewicz, Katarzyna, Jozkowicz, Alicja & Dulak, Jozef (2015). The role of oxidative stress in skeletal muscle injury and regeneration: focus on antioxidant enzymes. *Journal of muscle research and cell motility*, *36*(6), 377–393, doi: 10.1007/s10974-015-9438-9.

Larsson, Lars, Degens, Hans, Li, Meishan, Salviati, Leonardo, Lee, Young Il, Thompson, Wesley, Kirkland, James L. & Sandri, Marco (2018). Sarcopenia: Aging-Related Loss of Muscle Mass and Function. *Physiological reviews*, *99*(1), 427–511, doi: 10.1152/physrev.00061.2017.

Le Moal, Emmeran, Pialoux, Vincent, Juban, Gaëtan, Groussard, Carole, Zouhal, Hassane, Chazaud, Bénédicte & Mounier, Rémi (2017). Redox Control of Skeletal Muscle Regeneration. *Antioxidants & redox signaling*, *27*(5), 276–310, doi: 10.1089/ars.2016.6782.

Lei, Hui-Min, Zhang, Ke-Ren, Wang, Cong Hui, Wang, Yang, Zhuang, Guang-Lei, Lu, Li-Ming, Zhang, Jian, Shen, Ying, Chen, Hong-Zhuan & Zhu, Liang (2019). Aldehyde dehydrogenase 1A1 confers erlotinib resistance via facilitating the reactive oxygen species-reactive carbonyl species metabolic pathway in lung adenocarcinomas. *Theranostics*, *9*(24), 7122–7139, doi: 10.7150/thno.35729.

Lin, Liz Zhe & Lin, Jianqing (2011). Antabuse (disulfiram) as an affordable and promising anticancer drug. *International journal of cancer*, *129*(5), 1285-6; author reply 1286-7, doi: 10.1002/ijc.25780.

Liu, Xinwei, Wang, Lihui, Cui, Wei, Yuan, Xiangzhong, Lin, Lulu, Cao, Qi, Wang, Nannan, Li, Yi, Guo, Wei, Zhang, Xun, Wu, Chunfu & Yang, Jingyu (2016). Targeting ALDH1A1 by disulfiram/copper complex inhibits non-small cell lung cancer recurrence driven by ALDH-positive cancer stem cells. *OncoTarget*, *7*(36), 58516–58530, doi: 10.18632/oncotarget.11305.

Mackey, Abigail L., Rasmussen, Lotte K., Kadi, Fawzi, Schjerling, Peter, Helmark, Ida C., Ponsot, Elodie, Aagaard, Per, Durigan, João Luiz Q. & Kjaer, Michael (2016). Activation of satellite cells and the regeneration of human skeletal muscle are expedited by ingestion of nonsteroidal anti-inflammatory medication. *FASEB journal : official publication of the Federation of American Societies for Experimental Biology*, *30*(6), 2266–2281, doi: 10.1096/fj.201500198R.

Montarras, Didier, L'honoré, Aurore & Buckingham, Margaret (2013). Lying low but ready for action: the quiescent muscle satellite cell. *The FEBS journal*, *280*(17), 4036–4050, doi: 10.1111/febs.12372.

Monti, Eugenio & Fanzani, Alessandro (2016). Uncovering metabolism in rhabdomyosarcoma. *Cell cycle (Georgetown, Tex.)*, *15*(2), 184–195, doi: 10.1080/15384101.2015.1071746.

Moran, Jennifer L., Li, Yizheng, Hill, Andrew A., Mounts, William M. & Miller, Christopher P. (2002). Gene expression changes during mouse skeletal myoblast differentiation revealed by transcriptional profiling. *Physiological genomics*, *10*(2), 103–111, doi: 10.1152/physiolgenomics.00011.2002.

Moriarty, John D. (1950). THE USE OF ANTABUS IN THE THERAPY OF ALCOHOLIC PATIENTS. *California Medicine*, *73*(2), 144–147. PMID: 15426987

Motohashi, Norio, Asakura, Yoko & Asakura, Atsushi (2014). Isolation, culture, and transplantation of muscle satellite cells. *Journal of visualized experiments : JoVE.* Advance online publication, doi: 10.3791/50846.

Mukund, Kavitha & Subramaniam, Shankar (2020). Skeletal muscle: A review of molecular structure and function, in health and disease. *Wiley interdisciplinary reviews. Systems biology and medicine*, *12*(1), e1462, doi: 10.1002/wsbm.1462.

Musarò, Antonio, Fulle, Stefania & Fanò, Giorgio (2010). Oxidative stress and muscle homeostasis. *Current opinion in clinical nutrition and metabolic care*, *13*(3), 236–242, doi: 10.1097/MCO.0b013e3283368188.

Nelke, Christopher, Dziewas, Rainer, Minnerup, Jens, Meuth, Sven G. & Ruck, Tobias (2019). Skeletal muscle as potential central link between sarcopenia and immune senescence. *EBioMedicine*, *49*, 381–388, doi: 10.1016/j.ebiom.2019.10.034.

Papaconstantinou, J., Wang, C. Z., Zhang, M., Yang, S., Deford, J., Bulavin, D. V. & Ansari, N. H. (2015). Attenuation of p38α MAPK Stress Response Signaling Delays the in Vivo Aging of Skeletal Muscle Myofibers and Progenitor Cells. *Aging*, *7*(9), doi: 10.18632/aging.100802.

Portiér, G. L., Benders, A. G., Oosterhof, A., Veerkamp, J. H. & van Kuppevelt, T. H. (1999). Differentiation markers of mouse C2C12 and rat L6 myogenic cell lines and the effect of

the differentiation medium. *In vitro cellular & developmental biology. Animal*, *35*(4), 219–227, doi: 10.1007/s11626-999-0030-8.

Pownall, Mary Elizabeth, Gustafsson, Marcus K. & Emerson, Charles P. (2002). Myogenic regulatory factors and the specification of muscle progenitors in vertebrate embryos. *Annual review of cell and developmental biology*, *18*, 747–783, doi: 10.1146/annurev.cellbio.18.012502.105758.

Rajendran, Peramaiyan, Alzahrani, Abdullah M., Hanieh, Hamza N., Kumar, Sekar Ashok, Ben Ammar, Rebai, Rengarajan, Thamaraiselavan & Alhoot, Mohammed A. (2019). Autophagy and senescence: A new insight in selected human diseases. *Journal of cellular physiology*, *234*(12), 21485–21492, doi: 10.1002/jcp.28895.

Schiaffino, Stefano, Dyar, Kenneth A., Ciciliot, Stefano, Blaauw, Bert & Sandri, Marco (2013). Mechanisms regulating skeletal muscle growth and atrophy. *The FEBS journal*, *280*(17), 4294–4314, doi: 10.1111/febs.12253.

Schieber, Michael & Chandel, Navdeep S. (2014). ROS Function in Redox Signaling and Oxidative Stress. *Current Biology*, *24*(10), R453-R462, doi: 10.1016/j.cub.2014.03.034.

Shefer, Gabi, Rauner, Gat, Stuelsatz, Pascal, Benayahu, Dafna & Yablonka-Reuveni, Zipora (2013). Moderate-intensity treadmill running promotes expansion of the satellite cell pool in young and old mice. *The FEBS journal*, *280*(17), 4063–4073, doi: 10.1111/febs.12228.

Shen, X., Collier, J. M., Hlaing, M. & Zhang, L., et al. (2003). Genome-wide examination of myoblast cell cycle withdrawal during differentiation. *Developmental dynamics : an official publication of the American Association of Anatomists*, *226*(1), 128–138, doi: 10.1002/dvdy.10200.

Sin, T. K., Pei, X. M., Teng, B. T., Tam, E. W., Yung, B. Y. & Siu, P. M. (2013). Oxidative Stress and DNA Damage Signalling in Skeletal Muscle in Pressure-Induced Deep Tissue Injury. *Pflugers Archiv: European journal of physiology*, *465*(2), doi: 10.1007/s00424-012-1205-9.

Singh, Surendra, Brocker, Chad, Koppaka, Vindhya, Chen, Ying, Jackson, Brian C., Matsumoto, Akiko, Thompson, David C. & Vasiliou, Vasilis (2013). Aldehyde dehydrogenases in cellular responses to oxidative/electrophilic stress. *Free radical biology & medicine*, *56*, 89–101, doi: 10.1016/j.freeradbiomed.2012.11.010.

Snijders, Tim, Nederveen, Joshua P., McKay, Bryon R., Joanisse, Sophie, Verdijk, Lex B., van Loon, Luc J. C. & Parise, Gianni (2015). Satellite cells in human skeletal muscle plasticity. *Frontiers in Physiology*, *6, doi: 10.3389/fphys.2015.00283*.

Soprano, Dianne Robert, Teets, Bryan W. & Soprano, Kenneth J. (2007). Role of Retinoic Acid in the Differentiation of Embryonal Carcinoma and Embryonic Stem Cells. In G. Litwack (Hg.), *Vitamins and hormones: Bd. 75.2007. Vitamin A: Vitamins and hormones advances in research and applications* (Bd. 75, S. 69–95). Elsevier, Acad. Press.

Sousa-Victor, P., Gutarra, S., García-Prat, L., Rodriguez-Ubreva, J., Ortet, L., Ruiz-Bonilla, V., Jardí, M., Ballestar, E., González, S., Serrano, A. L., Perdiguero, E. & Muñoz-Cánoves, P. (2014). Geriatric Muscle Stem Cells Switch Reversible Quiescence Into Senescence. *Nature*, *506*(7488), doi: 10.1038/nature13013.

Takaki, Akinobu, Kawano, Seiji, Uchida, Daisuke, Takahara, Masahiro, Hiraoka, Sakiko & Okada, Hiroyuki (2019). Paradoxical Roles of Oxidative Stress Response in the Digestive System before and after Carcinogenesis. *Cancers*, *11*(2), doi: 10.3390/cancers11020213.

Thornell, Lars-Eric (2011). Sarcopenic obesity: satellite cells in the aging muscle. *Current opinion in clinical nutrition and metabolic care*, *14*(1), 22–27, doi: 10.1097/MCO.0b013e3283412260.

Tierney, Matthew T. & Sacco, Alessandra (2016). Satellite Cell Heterogeneity in Skeletal Muscle Homeostasis. *Trends in cell biology*, *26*(6), 434–444, doi: 10.1016/j.tcb.2016.02.004.

Tomita, Hiroyuki, Tanaka, Kaori, Tanaka, Takuji & Hara, Akira (2016). Aldehyde dehydrogenase 1A1 in stem cells and cancer. *OncoTarget*, *7*(10), 11018–11032, doi: 10.18632/oncotarget.6920.

Vainshtein, Anna & Hood, David A. (2016). The regulation of autophagy during exercise in skeletal muscle. *Journal of applied physiology (Bethesda, Md. : 1985)*, *120*(6), 664–673, doi: 10.1152/japplphysiol.00550.2015.

van Deursen, Jan M. (2014). The role of senescent cells in ageing. *Nature*, *509*(7501), 439–446, doi: 10.1038/nature13193.

Vassalli, Giuseppe (2019). Aldehyde Dehydrogenases: Not Just Markers, but Functional Regulators of Stem Cells. *Stem cells international*, *2019*, 3904645, doi: 10.1155/2019/3904645.

Vauchez, Karine, Marolleau, Jean-Pierre, Schmid, Michel, Khattar, Patricia, Chapel, Alain, Catelain, Cyril, Lecourt, Séverine, Larghéro, Jérôme, Fiszman, Marc & Vilquin, Jean-Thomas (2009). Aldehyde dehydrogenase activity identifies a population of human skeletal muscle cells with high myogenic capacities. *Molecular therapy : the journal of the American Society of Gene Therapy*, *17*(11), 1948–1958, doi: 10.1038/mt.2009.204.

Vella, Joseph B., Thompson, Seth D., Bucsek, Mark J., Song, Minjung & Huard, Johnny (2011). Murine and human myogenic cells identified by elevated aldehyde dehydrogenase activity: implications for muscle regeneration and repair. *PloS one*, *6*(12), e29226, doi: 10.1371/journal.pone.0029226.

Wackerhage, H. (2017). Sarcopenia: Causes and Treatments. *Deutsche Zeitschrift für Sportmedizin*, *2017*(07-08), 178–184, doi: 10.5960/dzsm.2017.289.

Wall, Tamara L., Luczak, Susan E. & Hiller-Sturmhöfel, Susanne (2016). Biology, Genetics, and Environment: Underlying Factors Influencing Alcohol Metabolism. *Alcohol Research : Current Reviews*, *38*(1), 59–68. PMID: 27163368

Wang, Wenjun, Wang, Chunguang, Xu, Hongxin & Gao, Yanhang (2020). Aldehyde Dehydrogenase, Liver Disease and Cancer. *International journal of biological sciences*, *16*(6), 921–934, doi: 10.7150/ijbs.42300.

Wang, Yu Xin, Dumont, Nicolas A. & Rudnicki, Michael A. (2014). Muscle stem cells at a glance. *Journal of cell science*, *127*(Pt 21), 4543–4548, doi: 10.1242/jcs.151209.

Wang, Yu Xin & Rudnicki, Michael A. (2011). Satellite cells, the engines of muscle repair. *Nature reviews. Molecular cell biology*, *13*(2), 127–133, doi: 10.1038/nrm3265.

Wei, Yan, Li, Yuan, Chen, Chao, Stoelzel, Katharina, Kaufmann, Andreas M. & Albers, Andreas E. (2011). Human skeletal muscle-derived stem cells retain stem cell properties after expansion in myosphere culture. *Experimental Cell Research*, *317*(7), 1016–1027, doi: 10.1016/j.yexcr.2011.01.019.

Wen, Xin & Klionsky, Daniel J. (2016). Autophagy is a key factor in maintaining the regenerative capacity of muscle stem cells by promoting quiescence and preventing senescence. *Autophagy*, *12*(4), 617–618, doi: 10.1080/15548627.2016.1158373.

Wu, Wei, Schecker, Johannes, Würstle, Sylvia, Schneider, Fabian, Schönfelder, Martin & Schlegel, Jürgen (2018). Aldehyde dehydrogenase 1A3 (ALDH1A3) is regulated by autophagy in human glioblastoma cells. *Cancer Letters*, *417*, 112–123, doi: 10.1016/j.canlet.2017.12.036.

Wu, Wei, Wu, Yang, Mayer, Karoline, Rosenstiel, Charlotte von, Schecker, Johannes, Baur, Sandra, Würstle, Sylvia, Liesche-Starnecker, Friederike, Gempt, Jens & Schlegel, Jürgen (2020). Lipid Peroxidation Plays an Important Role in Chemotherapeutic Effects of Temozolomide and the Development of Therapy Resistance in Human Glioblastoma. *Translational oncology*, *13*(3), 100748, doi: 10.1016/j.tranon.2020.100748.

Yablonka-Reuveni, Zipora (2011). The skeletal muscle satellite cell: still young and fascinating at 50. *The journal of histochemistry and cytochemistry : official journal of the Histochemistry Society*, *59*(12), 1041–1059, doi: 10.1369/0022155411426780.

Zhang, Chujing, Amanda, Stella, Wang, Cheng, Tan, Tze King, Ali, Muhammad Zulfaqar, Leong, Wei Zhong, Ng, Ley Moy, Kitajima, Shojiro, Li, Zhenhua, Yeoh, Allen Eng Juh, Tan, Shi Hao & Sanda, Takaomi (2020). Oncorequisite role of an aldehyde dehydrogenase in the pathogenesis of T-cell acute lymphoblastic leukemia. *Haematologica.* Advance online publication, doi: 10.3324/haematol.2019.245639.

Zuo, Li & Pannell, Benjamin K. (2015). Redox Characterization of Functioning Skeletal Muscle. *Frontiers in Physiology*, *6, doi: 10.3389/fphys.2015.00338*.

I. List of Tables

J. List of Figures

K. Appendix Material

1. Chemical and reagent

Table 24: Chemical and Reagent

Substances	Catalog Number	Company
ABC HRP Kit	PK-4000	Vector Laboratories
Acetic Acid	7332.1	Carl Roth GmbH
Acrylamide	3029.1	Carl Roth GmbH
Aldefluor Assay Kit	01700	Stemcell Technologies
Ammonium peroxodisulfate (APS)	9592.2	Carl Roth GmbH
Ampicillin	A9393	Sigma Aldrich
Bbsl restriction enzyme	R0539S	New England Biolabs GmbH
Biozym LE Agarose	840002	Biozym Scientific GmbH
Bromphenol-blue	B0126	Sigma Aldrich
BSA	8076.4	Carl Roth GmbH
Collagen I, rat tail	A1048301	Life Technologies
Collagenase XI (Closridium histolyticum)	C9407	Sigma Aldrich
Corning Matrigel	7340270	VWR
DAPI	SP-8500	Vector

Dimethylsulfoxide (DMSO)	A994.2	Carl Roth GmbH
Disulfiram	D2950000	Sigma Aldrich
Dithiothreitol (DTT)	ab141390	Abcam
DNase I	LK003172	CellSystems Biotechnology
Donkey Serum	D9663	Sigma Aldrich
Ethanol	T171.1	Carl Roth GmbH
Formaldehyde Solution	252549	Carl Roth GmbH
G418	N6386-5G	Sigma Aldrich
Gelatine from cold water fish	G7047	Sigma Aldrich
Glycerol	G5516	Carl Roth GmbH
Glycine	3790.3	Carl Roth GmbH
Hoechst 33342 Solution	H21492	Thermo Fisher Scientific
Horse Serum	S-2000	Vector Laboratories
LB Medium Powder	12795027	Thermo Fisher Scientific
Lipofectamine 3000	L3000008	Thermo Fisher Scientific
Mounting Medium	H-1000	Vectashield
NEB 5-alpha competent E.coli	C2987H	New England Biolabs GmbH
NEBuffer2	B7002S	New England Biolabs GmbH
Page Ruler Plus	26619	Thermo Fisher Scientific

Ponceau S	5938.1	Carl Roth GmbH
Propidium iodide solution	P4864	Carl Roth GmbH
Protease (Streptomyces griseus)	P8811	Sigma Aldrich
Protease/ Phosphatase inhibitor cocktail (100X)	5872	Cell Signaling Technology
Immobilon-P Membrane, PVDF	IPVH00010	Millipore, Merck
RNeasy mini kit	74204	Qiagen
Senescence Detection Kit	9860	Cell Signaling
Sodium azide	S2002	Sigma Aldrich
Sodium chloride (NaCl)	9265.3	Carl Roth GmbH
Sodium dodecyl sulfate (SDS)	2326.2	Carl Roth GmbH
Sodium hydroxide 45% (NaOH)	0993.1	Carl Roth GmbH
Sodium hydroxide 2N (NaOH)	T135.1	Carl Roth GmbH
T4 DNA Ligase Buffer (10x)	B69	Thermo Fisher Scientific
T4 Polynucleotide kinase	EK0031	Thermo Fisher Scientific
Temed	2367.3	Carl Roth GmbH
Tris	0188.3	Carl Roth GmbH
Triton-X-100	3051.3	Carl Roth GmbH
Tween-20	9127.2	Carl Roth GmbH

2. Device and Software

Table 25: Device and Analysis Software

Software Name	Software Producer
Aperio ImageScope	Leica Biosystems
AxioVision 4.8.	Carl Zeiss Microscopy
Excel 2016	Microsoft Office
FlowJo 10	Tree Star
NanoDrop	Thermo Scientific
NIS-Elements Camera	Nikon
Word 2016	Microsoft Office

3. Technical Device

Table 26: Technical Device

Device	Model Number	Company
60°C Incubator	INB 200	Memmert GmbH
96-well plates cooler	Z606634-1EA	Eppendorf AG
Autoclave	VX-120	Memmert GmbH
Centrifuge	5417R 5425	Eppendorf AG
CO2 Incubator	HERAcells 150i	Thermo Fisher Scientific
Flow Cytometer	FACS Calibur	Becton Dickinson

Fluorescence Microscope	HBO 100	Carl Zeiss AG
Freezing Containers	CoolCell LX	Biocision
Gel Imaging System	E-Box CX5	Peqlab
Heat-Mixer	53355	Eppendorf AG
Inverted Microscope	TS100	Nikon
Microcentrifuge	063089 (1R)	Eppendorf AG
Mini Cooler	C12R	A. Hartenstein
Multi-Axle-Rotating-Mixer	CATA60207-70	VWR
pH-Meter	EL-20	Mettler Toledo
Power Supply	PowerPac 300	Bio-Rad Laboratories
Shaker	Minishaker MS1	IKA Werke GmbH
Spectrophotometer	NanoDrop 2000c	Thermo Fisher Scientific
Thermal Cycler	22331	Eppendorf AG
AI680 Imager	29270769	Amersham, GE Healthcare

L. Publications

1. Laura Rihani, Friederike Liesche-Starnecker, Jürgen Schlegel. Human skeletal muscle satellite cells co-express Aldehyde Dehydrogenase isoforms ALDH1A1 and ALDH1A3 (submitted to **Cells Tissues Organs**)

2. Laura Rihani, Sophie Franzmeier, Wei Wu, Jürgen Schlegel. Aldehyde Dehydrogenase 1 isoforms 1A1 and 1A3 are essential for myogenic differentiation (submitted to **Skeletal Muscle**)